

POLITECNICO DI TORINO

Master Degree Course in Biomedical Engineering



Master Degree Thesis

**Quantitative assessment of lower
limb bradykinesia in Parkinson's
disease patients using smartphone
sensors.**

Supervisors:

Prof. Gabriella OLMO

Prof. Monica VISINTIN

Author:

Stefano SIBILLE

September, 2018

Abstract

In a perspective of *evidence-based* medicine, data from measurement systems, processed by data mining techniques, can provide quantitative measures that can make the available clinical information more objective and be an important aid for clinical decision making. This is the *leitmotif* of this project.

In this Master Thesis work the focus is on motor symptoms of Parkinson's disease, in particular on bradykinesia (slowness of movement). The motivation is found in the need to have quantitative methods for the motor assessment of patients, in order to be able to monitor the daily fluctuations of the motor symptoms (alternate of phase ON and phase OFF). In fact, the most used clinical evaluation scale, the MDS-UPDRS, in which the clinician is asked to assign a score between 0 and 4 according to the severity of the considered symptom, does not meet requirements of objectivity and repeatability. Furthermore, the fact that this kind of evaluation is performed only within follow-up sessions make impossible for the neurologist to observe the variations of the pharmacological/surgical treatment that occurs in Parkinson's disease patients.

The main techniques for the assessment of motor functions in Parkinson's disease, based on inertial sensors located in wearable devices, were analysed in literature. The purpose of this study is to investigate the use of a common smartphone to collect data during the execution of a motor task and the best machine learning method for the quantitative assessment of bradykinesia.

Ninety-three Parkinson's disease patients and ten healthy people participated in this study. The data used in the project was gathered from a smartphone positioned on the thigh while the patient conducted a prescribed movement activity: the Leg Agility (task 3.8 in the MDS-UPDRS). Some machine learning models were trained and tested for the supervised classification based on the UPDRS scale. A set of 16 features were extracted from the data and both multiclass classification and binary classification were performed.

Aknowledgements

I would first like to thank my supervisors Prof. Gabriella Olmo for her constructive suggestions and for providing a pleasurable working atmosphere and Prof. Monica Visintin for her valuable guidance.

I would like to express my sincere gratitude to all the expert neurologists of the Parkinson's disease and movement disorders Centre in Molinette Hospital (Turin), coordinated by Prof. Lopiano. My special thanks are addressed to Dr. Zibetti, Dr. Fabbri, Dr. Romagnolo, Dr. Rizzone, Dr. Bonvegna, Dr. Cormio and Dr. Artusi. This work would not have been realized without their passionate participation, their precious advice and their strong support.

I would also like to thank the members of the *Associazione Amici Parkinsoniani Piemonte Onlus* (city of Turin) and the people of *Casa di Riposo Orfanelle* (city of Chieri, Turin) for the time they gave us.

I am exceptionally grateful to my friends for supporting me throughout these years and for all the great moments shared together.

Last, but not least, I wish to thank my parents and my brother for their love and encouragement throughout my studies. My grandparents, cousins, aunties and uncles deserve my heartfelt thanks as well.

Contents

Abstract	I
Acknowledgements	II
Introduction	1
1 Parkinson's Disease	4
1.1 History and Epidemiology	4
1.2 Pathophysiology and Risk Factors	5
1.3 Symptoms and Causes	6
1.4 A focus on bradykinesia	8
1.5 Functional neuroimaging	9
1.6 Pharmacological treatment	10
1.7 Surgical treatment	12
1.8 The Unified Parkinson's Disease Rating Scale (UPDRS)	13
1.9 Lower limbs motor evaluation: Leg Agility Task	14
2 Smartphone inertial sensors	15
Introduction	15
2.1 MEMS Accelerometer	16
2.2 MEMS Gyroscope	17
2.3 Sensor Log App	19
3 Methods	20
3.1 Available data from PD population	20
3.2 Available data from Control population	21
3.3 Protocol	21
3.4 Pre-processing	22
3.5 Defined features	22
3.5.1 Number of movements	24
3.5.2 Mean time interval between movements	24

3.5.3	Standard deviation of the time intervals	25
3.5.4	Thigh inclination trend	25
3.5.5	Mean and max value of thigh inclination	26
3.5.6	Maximum acceleration and angular velocity	26
3.5.7	Range of acceleration and angular velocity	26
3.5.8	Root Mean Square value	26
3.5.9	Signal Entropy	27
3.5.10	Dominant Frequency Component	27
3.5.11	Ratio of dominant frequency power to total power	28
3.6	Machine learning algorithms	29
3.6.1	Training and validation of methods	30
3.6.2	k-Nearest Neighbor (kNN)	31
3.6.3	Support Vector Machine (SVM)	32
3.6.4	Neural networks (NN)	33
3.6.5	Decision trees	35
3.6.6	Linear Discriminant Analysis (LDA)	35
3.7	Hypothesis for feature set	36
3.7.1	Hypothesis 1: All available features	36
3.7.2	Hypothesis 2: Features from accelerometer	36
3.7.3	Hypothesis 3: Features from gyroscope	36
3.8	Statistical and performance descriptors	36
3.8.1	Boxplot	36
3.8.2	Confusion Matrix	37
4	Results	39
4.1	Examples of angular velocity signals	39
4.2	Examples of accelerometer signals	40
4.3	Boxplots	41
4.4	Hypothesis 1: All available features	43
4.5	Hypothesis 2: Features from accelerometer	46
4.6	Hypothesis 3: Features from gyroscope	49
4.7	Binary classification	51
4.8	Control population results	52
5	Discussion	53
6	Conclusion	55
A	Parkinson's disease and Control population details	56
	Bibliography	60

List of Figures

1.1	Levels of dopamine in a PD neuron (right) and normal levels (left). From [16].	5
1.2	Location of <i>Substantia Nigra</i> in the human brain [17]	6
1.3	^{123}I SPECT images of a healthy control (left) and a patient with Parkinson's disease (right). PD patient shows bilateral but asymmetric loss of putamen DAT binding. [31]	10
2.1	Sketch of a MEMS accelerometer (a) and sensor axis orientation (b).	17
2.2	Apparent path deflection due to Coriolis effect.	18
2.3	Smartphone rotation axes.	18
2.4	Sensor Log app interface (a) and list of selected sensors (b).	19
3.1	Smartphone position adopted for the Leg Agility task.	21
3.2	Distribution of the UPDRS scores assigned to the Leg Agility tasks.	22
3.3	Raw and bandpass filtered gyroscope measurements of the left leg of patient 64.	23
3.4	Peaks found by ready-made function <code>findpeaks</code> . Example of UPDRS 0 (a) and UPDRS 3 (b)	24
3.5	Pitch signal from a patient showing a clear decrement in amplitude.	25
3.6	Illustration of the procedure of cross-validation. For each iteration, one fold is left out and used as a test set, while the other folds are used combined as a training set.	30
3.7	Basic principle of kNN classification method. From [57]	32
3.8	Two linearly separable datasets with the hyperplane which maximizes the distance between the two groups of data. From [60]	33
3.9	Artificial Neural Network architecture. From [62]	34
3.10	Decision tree classifier architecture. From [65]	35

3.11	A boxplot with its terminology.	37
3.12	A confusion matrix for a binary classifier and its terminology.	38
3.13	A confusion matrix for a multiclass classification problem.	38
4.1	Time trajectories of x-axis angular velocity from UPDRS 0 to 4.	40
4.2	Time trajectories of z-axis acceleration from UPDRS 0 to 4.	41
4.3	Boxplot showing a trend of both the maximum acceleration value (a) and the range of the signal values (b) along with the severity of the symptom.	42
4.4	Boxplot showing a trend of both the maximum angular velocity value (a) and the range of the signal values (b) along with the severity of the symptom.	42
4.5	Boxplot of the mean time interval between movements (a) and the dominant frequency (b).	43
4.6	Confusion matrix based on the results from the Linear SVM classification model. The blue cell in the bottom right displays the overall correct classification percentage and incorrect classification percentage. The correctly classifies case are positioned diagonally (green) while the misclassifies cases are places in the other cells (red).	44
4.7	Confusion matrices based on the results from the kNN classification model.	45
4.8	Confusion matrix based on the results from the Linear Discriminant Analysis (LDA) model.	45
4.9	Confusion matrix based on the results from the Decision Tree model.	46
4.10	Confusion matrix based on the results from the supervised Neural Network model for Hypothesis 1.	47
4.11	Confusion matrices based on the results from the SVM (a) and kNN (b) classification models for Hypothesis 2.	47
4.12	Confusion matrices based on the results from the Linear Discriminant Analysis (a) and Decision Tree (b) classification models for Hypothesis 2.	48
4.13	Confusion matrix based on the results from the supervised Neural Network model for Hypothesis 2.	48
4.14	Confusion matrices based on the results from the SVM (a) and kNN (b) classification models for Hypothesis 3.	49
4.15	Confusion matrices based on the results from the Linear Discriminant Analysis (a) and Decision Tree (b) classification models for Hypothesis 3.	50

4.16	Confusion matrix based on the results from the supervised Neural Network model for Hypothesis 3.	50
4.17	Confusion matrix based on the results from the supervised Neural Network model.	51
4.18	Confusion matrices based on the results from the kNN (a) and SVM (b) classification models.	52

List of Tables

3.1	PD patients' demographic and clinical characteristics.	20
3.2	List of features used in this thesis work.	23
4.1	Correct classification percentage of the selected classification methods for each UPDRS class and overall performance. The best results come from Neural Networks (gray line).	43
4.2	Classification of control population signals.	52
A.1	Parkinson's disease population recruited in this thesis work.	56
A.2	Control population recruited in this thesis work.	59

List of Acronyms

DBS Deep Brain Stimulation

FDA Food and Drug Administration

LA Leg Agility

LDA Linear Discriminant Analysis

kNN k-Nearest Neighbor

MDS Movement Disorder Society

MEMS Micro Electro-Mechanical Systems

ML Machine Learning

NN Neural Network

PD Parkinson's Disease

RBD REM Behavior Disorder

SVM Support Vector Machine

UPDRS Unified Parkinson's Disease Rating Scale

Introduction

According to the Italian Parkinson's Association, more than 300 000 people are living with Parkinson's disease in Italy [1]. Parkinson's disease patients present highly variable motor symptoms including bradykinesia (slowness of movements), postural instability, tremor and freezing of gait. The variability of symptoms needs a correctly adjusted medication. This is hard to achieve since the current state of the art for assessing PD symptoms in clinical routine is by using clinical rating scales based on observations and judgments of clinicians and medical history. In other words, there are no way of measuring the severity of motor symptoms other than listening to and observing the patient. This leads to the undesirable situation of a physician's assessment depending mainly on the display of symptoms within a very short time frame. This especially becomes a problem for long-term patients since the effect of the medication wears off after several years of usage. Additionally, similar symptoms may be rated differently depending on the physician's training and experience.

Consequently, a need for objective evaluation of patient symptoms outside of the short meeting between the patient and the physician is present. Therefore, the development of technical aids for short- and long-term objective symptom evaluation in both the clinical and the home environment is necessary in order to improve the treatment of each patient. Recently, several research groups have successfully quantified symptoms using accelerometers and gyroscopes ([2, 3, 4, 5, 6, 7]).

This thesis is a part of a larger project trying to develop easier and more objective tools for Parkinson's disease symptoms evaluation and monitoring. The main focus of this thesis work is to find the most suitable model structure for the quantification of bradykinesia in Parkinson's patients. It involves using machine learning techniques to quantify the data collected from smartphone sensors and train different classification algorithms to evaluate their performance with respect to diagnosing Parkinson's bradykinesia of lower limbs based on the Unified Parkinson's Disease Rating Scale (UPDRS).

Related work

Sensor-based PD motor symptoms analysis and quantification have got a lot of attention in the research field. Several research groups used data mining techniques and artificial intelligence systems to recognize the severity of motor symptoms using the data derived from wearable sensors.

Bonato et al [2] presented a preliminary evidence that the accelerometer and surface electromyographic signals recorded from PD patients during some motor tasks bring with them some features that can be used to correctly identify motor fluctuations. They show that data mining not only is able to classify these disorders for a correct patient assessment, but it has the potential of increasing our understanding of Parkinson's Disease disorders.

Patel et al [8] presented the results of a pilot study that aimed at assessing the feasibility of using accelerometer data to estimate the severity of tremor, bradykinesia and dyskinesia in parkinsonian patients. The expert clinicians were asked to score some standardized UPDRS motor tasks of twelve patients by analysing the video recordings of the movements and a comparison to the classification algorithm results was performed. They achieve average estimation error values of 3.4% for tremor, 2.2% for bradykinesia, and 3.2% for dyskinesia.

Heldman et al [9] developed and evaluated an algorithm for quantifying gait, freezing of gait and lower limb bradykinesia in PD patient using a heel-worn motion sensor unit. The aim of their study was to integrate the model into a home-based system for monitoring motor symptoms.

Kim et al [10] investigated and developed quantitative measures of lower limb bradykinesia.

Parisi et al [11] proposed an accurate description of the features for the characterization of the following motor tasks: Leg Agility, Sit-to-Stand and Gait. They commented the correlation between the kinematic variables and the UPDRS scoring.

Chapter 1

Parkinson's Disease

1.1 History and Epidemiology

Parkinson's disease (PD) is an idiopathic disease of the nervous system characterized by both motor and non-motor system manifestations. It is one of the most common chronic progressive neurodegenerative disorders, second only to Alzheimer's disease [12]. Although the physical symptoms and rudimentary medical descriptions date back thousands of years (e.g. by the medical researcher Galen of Pergamon in A.D. 175), one of the earliest clinical descriptions identifying PD as a neurologic syndrome is found in the 1800's when James Parkinson, a London surgeon, systematically described six individuals with symptoms of the disease that bears his name. In particular, in his "*An Essay on the Shaking Palsy*", published in 1817, for the first time he described the disease as:

Involuntary tremulous motion, with lessened muscular power, in parts not in action and even when supported; with a propensity to bend the trunk forwards, and to pass from a walking to a running pace: the senses and intellects being uninjured. [13]

However, it seems to have attracted little attention at the time. About six decades passed before the great French neurologist Jean-Martin Charcot spoke of the *maladie de Parkinson*.

According to the global declaration for PD, about 6.3 million people suffer from PD worldwide. The prevalence of PD is about 0.3% of the whole population in industrialized countries, rising up to 1% over the age of 65 and to 4% over 80 [14].

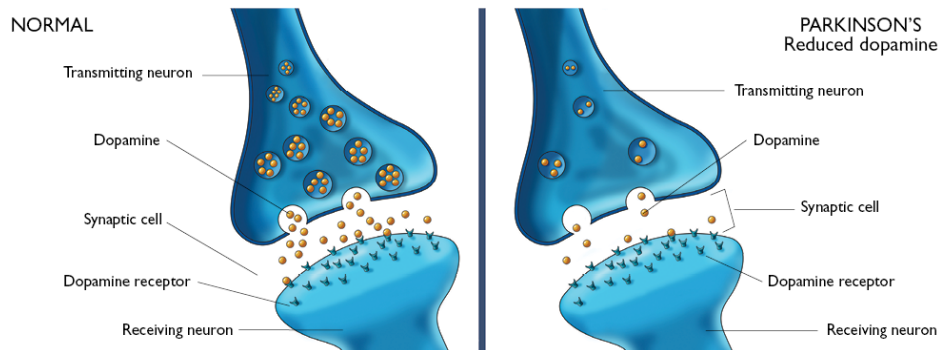


Figure 1.1: Levels of dopamine in a PD neuron (right) and normal levels (left). From [16].

1.2 Pathophysiology and Risk Factors

Although tremendous advances have been made in this field, PD is still considered largely idiopathic (i.e. of unknown cause). Physiologically, the symptoms associated with Parkinson's disease are the result of the loss of a number of neurotransmitters, most notably dopamine. Dopamine, like other neurotransmitters, transmits chemical messages from one nerve cell to another across the synapse, a space between the presynaptic cell and the postsynaptic receptor. Dopamine is secreted into the synapse from membrane storage vesicles in the presynaptic membrane. It crosses the synapse and binds to the postsynaptic membrane, where it activates dopamine receptors. Unused dopamine remaining in the synapse is absorbed back into the presynaptic cell; once back in the presynaptic cell, the excess dopamine is repackaged into storage vesicles and released once more into the synapse.

Although dopamine cell loss cannot be measured directly, measurements in neurologically normal people and in nonhuman primates reveal a slow progressive loss of dopamine with age. In Parkinson's disease the loss occurs at a much greater rate and both biochemical measures and imaging studies suggest that there is a significant decrease in dopamine by the time motor symptoms appear. Parkinson's disease can be described as an accelerated version of the cell death seen with normal aging. [15]

Figure 1.1 shows the difference between low dopamine levels in a neuron affected by PD and normal levels.

Degeneration of dopamine neurons is particularly evident in the area of the brainstem called *Substantia Nigra* (Fig. 1.2). As a result, dopamine avail-

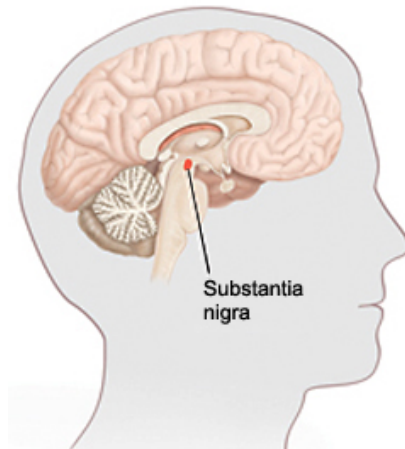


Figure 1.2: Location of *Substantia Nigra* in the human brain [17]

ability decreases and the symptoms progressively develop, becoming more severe over time. Aggregation of a protein that normally exists in the cells, called *alpha-synuclein*, is found in PD, forming round structures within the cell known as *Lewy bodies*. The factors and exact mechanisms that lead to the aggregation of *alpha-synuclein* and to the death of the dopaminergic neurons in PD are still not fully understood.

Most movement disorders specialists believe that PD results from a complex interplay between genetic predisposition and environmental factors. When the symptoms present at a younger age (below age 40), Parkinson's disease is often familial, caused primarily by genetic mutations.

1.3 Symptoms and Causes

Parkinson's disease symptoms and signs may vary from person to person. In the early stages signs may be mild and may go unnoticed for years. They can be divided into motor and non-motor, depending on whether they are related to body movement abnormalities or not. Onset of motor symptoms is asymmetric with usually an arm affected first. Signs and symptoms then spread to the other limb on that side and later affect the opposite side. The four cardinal motor symptoms are:

- **Bradykinesia:** a general slowing of movement, sometimes coupled with an inability to initiate it. Bradykinesia causes difficulties in performing sequential and repeated movements and, in the advanced stages, it is subject to rapid fluctuations from ease of movement to inability to move. To make an assessment, the doctor asks PD patients to

perform rapid, repetitive hand movements, such as tapping the index finger on the thumb and supination-pronation, or lower limb movements, such as raising and stomping the foot on the ground. Bradykinesia is present in all cases of Parkinson's;

- **Tremor:** an involuntary, rhythmical movement (at a frequency of approximately 4–6 Hz) that affects a part of the body. It is caused by the rapid and alternating contraction and relaxation of muscles. It is a resting tremor, which becomes more obvious and severe when the person is resting and improves with intentional movement [18]. It tends to be present in the hands, arms, legs, jaw and face. Tremor in the hand is typically of the "pill rolling" type, where the thumb and forefingers seem to rotate about the some point. Even if tremor is the most known motor symptom in Parkinson's disease, it is thought that approximately 70% of people with the condition have a tremor at the time of diagnosis;
- **Rigidity:** an abnormal stiffness in a limb or part of the body. Rigidity can prevent muscles from stretching and relaxing as they should. As a consequence, rigidity may be experienced as difficulty turning when walking, turning in bed and getting out of a chair or bed, as reduced arm swing when walking, difficulty with everyday activities such as dressing and writing, or as reduced facial expression or a mask-like face;
- **Postural instability:** an impaired balance and coordination or difficulty standing or walking. It also manifests as a stooped and droopy posture, as well as halts and freezes while walking [18]. People with advanced Parkinson's tend to walk with short, rapid steps (a behaviour called "festination"). This is one of the most disabling symptoms because of the increased chance of falls. To assess a patient's balance a trained movement disorder specialist gives a moderately forceful backwards tug on the patient and monitors how the patient recovers.

Resting tremor, bradykinesia and rigidity are relatively early signs often apparent in the first-affected extremity at the time of diagnosis. Postural instability or imbalance is a late symptom typically emerging several years into the disease [19].

Individuals with more progressive Parkinson's disease develop a distinctive shuffling walk with a diminished or absent arm swing. It may become difficult to start walking and to make turns. Individuals may freeze in mid-stride (Freezing of Gait) and appear to fall forward while walking.

A variety of non-motor symptoms have been described in the setting of Parkinson's disease:

Olfactory impairment is one of the most prevalent non-motor symptoms as it is present in more than 90% of patients with PD, often appearing at the very early stage of the disease [20]. Olfactory dysfunction is supposed to be associated to a more central deficit rather than a damage of the peripheral olfactory system [21].

Orthostatic hypotension is the most widely recognized aspect of cardiovascular dysfunction in PD. It may be present in almost 60% of patients, although only a minority of these patients may be symptomatic [22].

Constipation is another frequent non-motor sign in Parkinson's disease that can precede motor symptoms by more than 20 years [23]. About 70% - 80% PD patients suffer from it and it is reported that constipation is correlated with the severity and duration of the disease [24].

Sleep disturbances are very common in the setting of PD and their prevalence may reach close to 90%. One of the most frequent of them is the REM Sleep Behavior Disorder (RBD), in which an increased violent dream content leads to many violent and injurious movements, affecting also the caregivers' quality of life [25].

Other important non-motor symptoms include depression, urinary frequency, sexual dysfunction, sweating, hypersalivation, dysphagia, speech problems, hallucinations and fatigue [26].

1.4 A focus on bradykinesia

The term *bradykinesia* was first used by James Parkinson to describe a general slowness of movements. Although it is the most characteristic clinical feature in Parkinson's disease patients, it can be seen in many other disorders, including depression, Huntington's disease and dystonia [27].

Bradykinesia includes difficulties with planning and executing movements and with performing sequential and rapid tasks. The initial manifestation can be noticed in performing activities of daily living with slow movements and larger reaction times.

Bradykinesia is a term often used interchangeably with *akinesia* and *hypokinesia*. According to Merritt's Neurology [28], bradykinesia refers to a loss of automatic movement and difficult initiating it, hypokinesia is related

to a reduction in amplitude and difficulty with repetitive movements and akinesia is the loss of ability to move the muscles voluntarily (its typical sign is *freezing*).

Bradykinesia has many facets as it affects many body parts. Parkinson's disease patients' face loses spontaneous expression (*hypomimia*). The arms are characterized by loss of gesturing, the voice has a monotonous tone with a lack of inflection (*aprosody*) and the speech becomes very soft (*hypophonia*) and unclear (*dysarthria*). The dominant hand shows often a slow and small handwriting (*micrographia*).

Although secondary factors can contribute to bradykinesia (rigidity, tremor, muscle weakness), the primary deficit is caused by insufficient muscle force recruitment when initiating a movement [27].

Bradykinesia is the cardinal PD feature that correlates best with the degree of dopamine insufficiency [12], but it is supposed to be dependent on the emotional state of the patient. For example, excited patients may be able to make quick movements (such as suddenly run if the word "fire" is screamed). This behaviour is known as *kinesia paradoxa* and it suggests the integrity of the motor programmes in patients with PD but the difficulty in accessing them without an external trigger. It is well known that this deficit is ameliorated when external cues, such as a marching music or a loud noise, are given to guide the movement [12].

1.5 Functional neuroimaging

Since some patients, in particular in the very early stages of the disease, are hard to diagnose due to unclear clinical signs or unconvincing response to pharmacological treatment, a more accurate way to diagnose Parkinson's disease is a nuclear imaging technique. Assessment of the integrity of dopaminergic areas can be made using radio-labelled ligands, detected with SPECT (Single Photon Emission Computed Tomography) or PET (Positron Emission Tomography).

SPECT imaging using ^{123}I -Ioflupane (Brand name: DaTSCAN) is the most sensitive imaging technique and has proved useful in differentiating parkinsonism due to nigrostriatal degeneration and nondegenerative causes [29]. This technique is able to discriminate patients with neurodegenerative Parkinsonian Syndrome from healthy subjects or patients with tremor disorders (such as Essential tremor) by detecting presynaptic dopaminergic deficits. This type of imaging uses ^{123}I to bind to the DAT (dopamine transporter) and then the amount of transporter present is visualized. These

transporters normally function to reuptake dopamine from the synaptic cleft and they are reduced 50-70% in patients with Parkinson's disease [30]. Normal scans are characterized by symmetric and intense "comma"-shaped regions, due to DAT binding in the caudate nucleus and putamen on both hemispheres (Fig 1.3 - left image). Abnormal scans, on the other hand, show distortions or asymmetry of this shape (Fig 1.3 - right image).

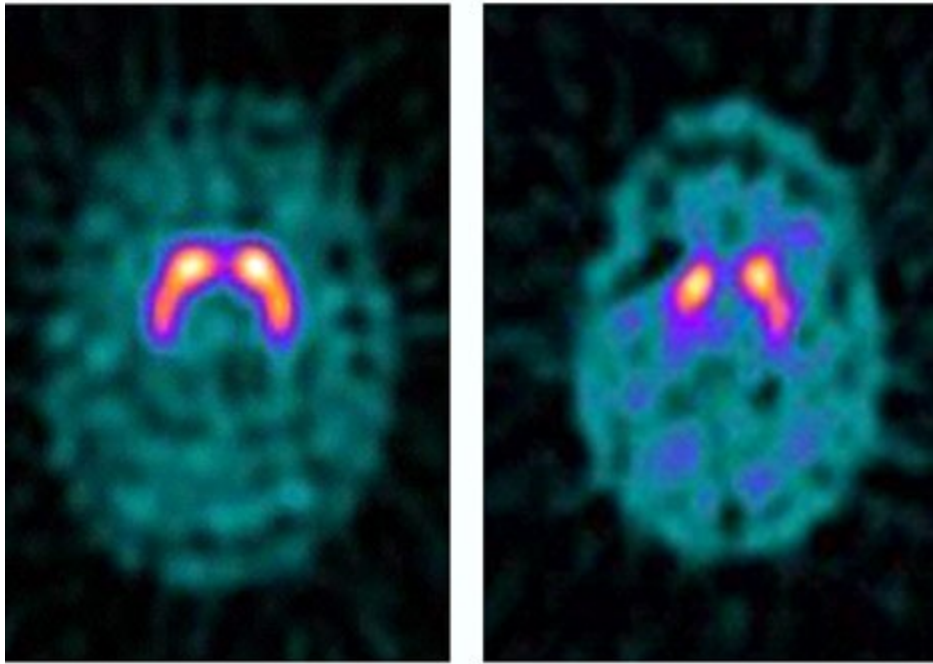


Figure 1.3: ^{123}I SPECT images of a healthy control (left) and a patient with Parkinson's disease (right). PD patient shows bilateral but asymmetric loss of putamen DAT binding. [31]

1.6 Pharmacological treatment

The goal of medical management of Parkinson's disease is to control signs and symptoms while minimizing side effects. In fact there are not neuroprotective therapies and, except in very early disease, medications will not entirely eliminate signs and symptoms [32]. As the disease progresses, symptoms increase despite best medical management [19].

The primary medication used to treat Parkinson's disease is levodopa. Dopamine itself is not effective as a medication because it cannot cross the blood-brain barrier, but levodopa is a dopamine precursor that can do so. Its

development in the late 1960s represents one of the most important breakthroughs in the history of medicine. Levodopa is administered with carbidopa, which prevents levodopa from being converted into dopamine prematurely in the bloodstream, allowing more of it to get to the brain. Therefore, a smaller dose of levodopa is needed to treat symptoms. The well-known combined carbidopa/levodopa name brand formulation is called Sinemet[®]. However, there are many different preparations of carbidopa/levodopa, including long-acting forms, a combined long and short-acting capsule called Rytary[®], a formulation that dissolves in the mouth without water, called Parcopa[®], and a combined formulation that includes the COMT inhibitor *entacapone*, called Stalevo[®].

Levodopa in pill form is absorbed in the blood from the small intestine and travels through the blood to the brain, where it is converted into dopamine. Carbidopa-levodopa immediate/extended release combination capsules (RytaryTM) maintain levodopa concentrations longer than the immediate-release or other available oral levodopa formulations. Following an initial peak at about one hour, plasma levodopa concentrations are maintained for about four to five hours before declining [33].

Carbidopa/levodopa is also available via a dopamine intestinal infusion pump (DuopaTM, approved by FDA in 2015). This solution is for patients with more advanced Parkinson's who still respond to carbidopa-levodopa, but who have a lot of fluctuations in their response. The small, portable infusion pump provides over 16 continuous hours of carbidopa and levodopa and delivers them directly into the small intestine. One of the major drawbacks to the pump approach is the need for a percutaneous gastrojejunostomy (i.e. a surgical procedure in which an anastomosis is created between the stomach and the proximal loop of the jejunum) [34]. The decision about when to start carbidopa/levodopa is different for every person with PD and requires consideration of potential benefits, risks and the availability of alternatives.

The combination of carbidopa and levodopa is the most effective agent available for the treatment of motor symptoms and prolongs the capacity to perform instrumental activities of daily living. However, its early use is associated with earlier development of dyskinesias (uncontrolled choreic or dystonic movements).

Other types of medications available to treat the symptoms of Parkinson's disease include:

Dopamine agonists. They mimic dopamine effects in the brain directly stimulating dopamine receptors and without changing into dopamine.

They last longer than levodopa and may be used to smooth the "on" and "off" effects. They include *pramipexole* (Mirapexin[®]), *ropinirole* (Requip[®]), *rotigotine* (Neupro[®], given as a patch) and *apomorphine*. Side effects of dopamine agonists include hallucinations, orthostatic hypotension, sleepiness and impulse control disorders (pathological gambling, compulsive shopping and eating, hyper-sexuality).

MAO B inhibitors. These medications inhibit the brain enzyme monoamine oxidase B (MAO B), which is an enzyme that metabolizes brain dopamine. They include *selegiline* (Jumex[®]), *rasagiline* (Azilect[®]) and *safinamide* (Xadago[®]).

COMT inhibitors. *entacapone* (Comtan[®]) is the primary medication for this class. Inhibitors of catechol-O-methyltransferase are commonly used as an adjunct to levodopa therapy for the amelioration of wearing-off symptoms [35].

Amantadine . It is a glutamate antagonist drug that can be prescribed to treat dyskinesias [36].

1.7 Surgical treatment

Surgical therapies are usually reserved for PD patients who are experiencing decreased effects of medical dopamine therapy over time. Specifically, continued motor fluctuations and dyskinesias may indicate candidacy. Motor fluctuations are manifested as alterations between good control "on" periods and PD symptomatic "off" periods.

Deep brain stimulation (DBS) is currently the mainstay surgical procedure for the treatment of advanced PD. This technique involves the surgical implantation of two leads with four contacts into the brain (accurately targeting specific structures within the basal ganglia like the subthalamic nucleus (STN), globus thalamus (GP) or ventral intermediate nucleus). The leads are connected by an extension wire that runs down the neck under the skin to a medical device (Implantable Pulse Generator, IPG) placed below the collarbone. The electrical impulses sent to these specific parts of the brain help improve the functioning of the motor pathways modifying firings of neurons in the target site. This procedure does not involve destruction of brain tissue, is reversible and can be adjusted as the disease progresses as well as bilateral procedures can be performed. The IPGs can be programmed for

monopolar stimulation (i.e. only one electrode is turned on) or bipolar (i.e. two to four electrodes are working). The pulse width, amplitude and current frequency can be adjusted by the expert neurologist using a hand held computer programmer placed on the skin over the stimulator.

As not all patients are candidates for surgical treatment, a careful patient assessment and selection by a movement disorders specialist is paramount [37]. Factors that predict a good response to surgery for advanced Parkinson's disease include good response to levodopa, few comorbidities, absence of cognitive impairment, and absence of (or well-controlled) depression [38].

1.8 The Unified Parkinson's Disease Rating Scale (UPDRS)

In the clinical field, the evaluation of the motor and non-motor impairments in PD is limited to the use of scales and questionnaires. The Unified Parkinson's Disease Rating Scale (UPDRS) has been the most widely used clinical rating scale for Parkinson's disease and the reference measure for regulatory agencies since its development in the 1980s [39]. In 2001, the Movement Disorder Society (MDS) sponsored a critique of the UPDRS and the summary conclusions recommended the development of a new version, termed the MDS-sponsored UPDRS revision (MDS-UPDRS). It retained the strengths of the original scale, but resolved identified problems and especially incorporated a number of clinically pertinent PD-related problems poorly captured in the original version. It consists of 42 items in four subscales:

- **Section I:** Non-motor experiences of daily living;
- **Section II:** Motor experiences of daily living;
- **Section III:** Motor examination for both sides and different body parts;
- **Section IV:** Motor complications (including dyskinesias and fluctuations).

The first half of Section I concerns a number of behaviors that are assessed by the investigator with all pertinent information from patients and caregivers. The second half of Section I and all the Section II are designed to be amenable to questionnaire format and therefore can be completed by the patient with or without the aid of the caregiver, but independently of the

investigator. In any case, these two sections can be reviewed by the investigator to ensure completeness and clarity, and also any perceived ambiguities can be explained. Section III retains the objective assessments of parkinsonism and all tasks have specific instructions to give or demonstrate to the patient. This section is completed by the examiner. Finally, for Section IV the investigator is required to conduct the interview.

Each question is anchored with five responses that are linked to commonly accepted clinical terms:

0 : **Normal**;

1 : **Slight** (i.e. symptoms/signs with sufficiently low frequency or intensity that cause no impact on function);

2 : **Mild** (i.e. symptoms/signs of frequency or intensity sufficient to cause a modest impact on function);

3 : **Moderate** (i.e. symptoms/signs sufficiently frequent or intense to impact considerably, but not prevent, function);

4 : **Severe** (i.e. symptoms/signs that prevent function).

1.9 Lower limbs motor evaluation: Leg Agility Task

A task specifically requested by the UDPRS scale for motor evaluation of lower limbs is the Leg Agility task (LA). It consists of raising and stomping the foot on the ground 10 times as high and as fast as possible, starting from a sitting posture. Each leg is tested separately. According to the guidelines of the Movement Disorder Society this task must be evaluated observing the following parameters: speed, amplitude, slowing, hesitations and interruptions.

Chapter 2

Smartphone inertial sensors

Introduction

Advancements in technology have always had major impacts in medicine. The smartphone is one of the most ubiquitous and dynamic trends in communication and it is one of the fastest growing sectors in the technology industry. Its role in medicine and education appears promising and exciting [40].

Several examples of the use of smartphones for patient monitoring are present in literature. By using the smartphone's GPS, one can track Alzheimer disease patients' movements and provide them medicine and food timing notifications [41]. The smartphone has also been used in rehabilitation after a coronary event or angioplasty for exercise sessions [42] or to interpret gait and balance of patients with movements disorders using accelerometer sensors [43]. Smartphone's sensors (accelerometer, gyroscope and magnetometer) have also been used as fall detection and prevention solutions [44], as well as Freezing-of-Gait monitor systems in patients affected by Parkinson's disease [45].

Micro-Electro-Mechanical Systems (MEMS) are mechanical and electro-mechanical elements developed in the recent 50 years through microfabrication techniques. Since their first applications in the '50s, MEMS technologies have progressively established a wide range of small, high performance and inexpensive sensors. They are able to sense and respond to many variables such as pressure, flow, position, motion, strain [46].

Telehealth, telemonitoring and mobile health (mHealth) sensor technologies enable remote monitoring and management of patients affected by chronic diseases, both at home and in outdoor environments. In healthcare facilities, sensors focus on medical screening such as point-of-care parameters

measurement device. Novel sensors for human biomedical signal acquisition, together with wireless connectivity and low power solutions, are generating new opportunities for wearable devices, which enable and guarantee continuous monitoring together with users' freedom of movement [47]. In the clinical field sensor technologies can represent a key element to assist decision-making process [46].

This chapter provides an overview of MEMS accelerometers and gyroscopes technology and describes their working principle.

2.1 MEMS Accelerometer

An accelerometer measures proper acceleration, which is the acceleration it experiences relative to free fall. Proper acceleration is not the same as coordinate acceleration, being the rate of change of velocity, i.e. the acceleration in a fixed coordinate system. [48]

For example, an accelerometer at rest will measure an acceleration due to Earth's gravity, (by definition: $g = 9.81 \text{ m/s}^2$). By contrast, accelerometers in free fall will measure zero.

Modern accelerometers are small Micro Electro-Mechanical Systems (MEMS). They can be seen as the simplest MEMS devices possible, consisting of little more than a proof mass suspended on a fixed frame by a spring. The mass deflects from its neutral position under the influence of external accelerations, generated by the motion of the sensor or by gravity. Most commonly, the deflection of the proof mass is measured using the capacitance difference between a set of fixed sensing plates and a set of beams attached to the proof mass. Figure 2.1a shows a sketch of a MEMS accelerometer. The modern-day smartphone is equipped with low-power three-axis linear accelerometer which measures acceleration in Linear, Transversal and Vertical directions (x-, y- and z-axis), as shown in Figure 2.1b.

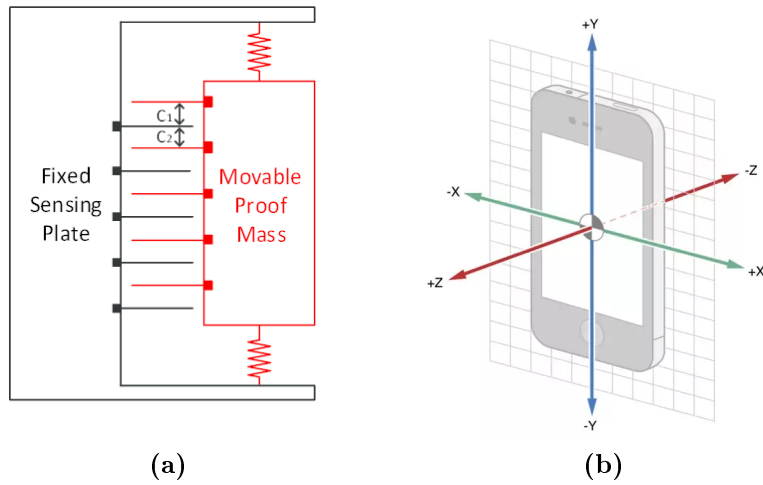


Figure 2.1: Sketch of a MEMS accelerometer (a) and sensor axis orientation (b).

2.2 MEMS Gyroscope

Gyroscope is a device that measures angular rotation by means of Coriolis acceleration, which is a result of Newton's law of motion applied to rotating frames. The Coriolis effect can be explained as follows, starting from Figure 2.2. On a rotating platform, a mass is subject to a linear vibratory motion. An observer in the same rotating frame rotates as the platform rotates and sees the mass as making a curvilinear movement instead of a linear one. This is due to the Coriolis force that causes a secondary vibration perpendicular to the primary vibration. However, for an observer outside the rotating frame, the mass is really making a single axis vibration. For this reason, Coriolis force is a *fictitious* or *inertial* force acting on a moving object in a rotating frame.

The vector formula for the magnitude and direction of the Coriolis force is derived through vector analysis and is:

$$\mathbf{F}_c = -2m\boldsymbol{\omega} \times \mathbf{v} \quad (2.1)$$

where m is the mass, $\boldsymbol{\omega}$ is the angular velocity vector with direction along the axis of rotation, \mathbf{v} is the linear velocity of the mass with respect to the rotating system and \times is the cross product operator.

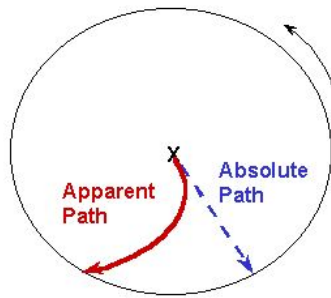


Figure 2.2: Apparent path deflection due to Coriolis effect.

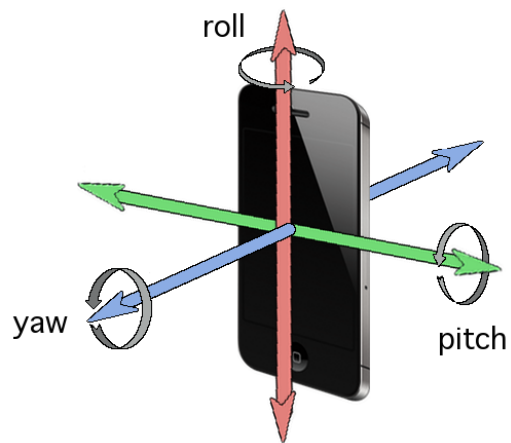


Figure 2.3: Smartphone rotation axes.

2.3 Sensor Log App

In this thesis work accelerometer and gyroscope data have been collected with an app called **Sensor Log** (Google Commerce, Ltd.) and exported in CSV format. This is only one of the various apps than can be used to acquire signals. Sensor Log has a very user-friendly interface, in which the user can add an "activity" button with all the sensors are expected to be useful. In this work, the "Leg Agility" (right leg and left leg) buttons are added. Fig 2.4 shows the app interface (a) and the list of sensors (b) chosen for this work's purpose. The user has to click on the button to start the acquisition and click again to end it. Then the signals are stored and appear like a database list in the "history" section of the app.

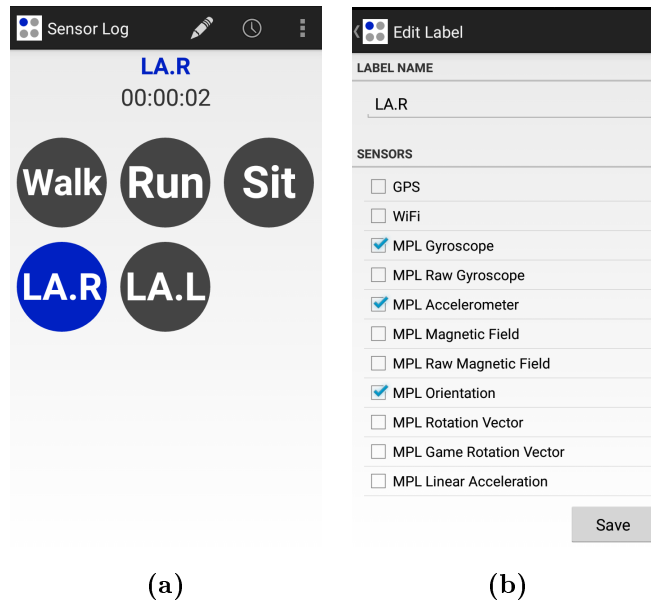


Figure 2.4: Sensor Log app interface (a) and list of selected sensors (b).

Chapter 3

Methods

This chapter describes the methods that have been used for analyzing the measured signals. Several PD related features have been extracted from the signals of both patients and healthy controls. All computations and signal processing were performed by using the MATLAB software and programming language (The MathWorks, Inc.).

3.1 Available data from PD population

A total number of ninety-three patients (mean age: 69, range: 43-87; mean age at diagnosis: 60.1, range: 29-81) were recruited in the study. Data have been collected between April and July 2018 in the outpatient clinic of the Parkinson’s disease and movement disorders Centre at Molinette Hospital (Turin) and in the offices of the *Associazione Amici Parkinsoniani Piemonte Onlus* in Turin. The inclusion criterion for patients was a clinical diagnosis of Parkinson’s Disease with motor symptoms. Table A.1 in the Appendix shows the details of PD population, while Table 3.1 illustrates a general overview.

Table 3.1: PD patients’ demographic and clinical characteristics.

Number of patients	Mean age (years \pm SD)	Years from PD diagnosis	Mean age at PD diagnosis (years \pm SD)
93 (70% male)	69 \pm 10	9.0 \pm 6,5	60.1 \pm 10.9

3.2 Available data from Control population

A total number of ten control people participated in this study. Most of the data have been collected in May 2018 in the nursing home *Orfanella* in the city of Chieri, Turin. Table A.2 in the Appendix shows the demographic details of the Control population.

3.3 Protocol

The subjects (PD patients and healthy people) were asked to sit in a straight-backed chair and place the foot on the ground in a comfortable position. Then, they had to perform the Leg Agility task from the MDS-UPDRS Motor Section with each leg separately. A simple Velcro armband with a smartphone inside (Samsung S5 mini) was placed around the patient's thigh, trying to have the y-axis of the smartphone as parallel as possible to the femur direction. Figure 3.1 shows the position adopted for all the participants.



Figure 3.1: Smartphone position adopted for the Leg Agility task.

As indicated in the UPDRS guidelines, the task was demonstrated to the subjects by the expert neurologist before patients performed it. The rater was asked to score each motor task according to the UPDRS scale in order

to use these ratings as class labels for the supervised classification algorithm. Figure 3.2 shows the distribution of the UPDRS scores assigned by all the expert neurologists.

Accelerometer and gyroscope data (sampling frequency: 200 Hz) have been collected and then exported in CSV format. All the data was processed offline using MATLAB software.

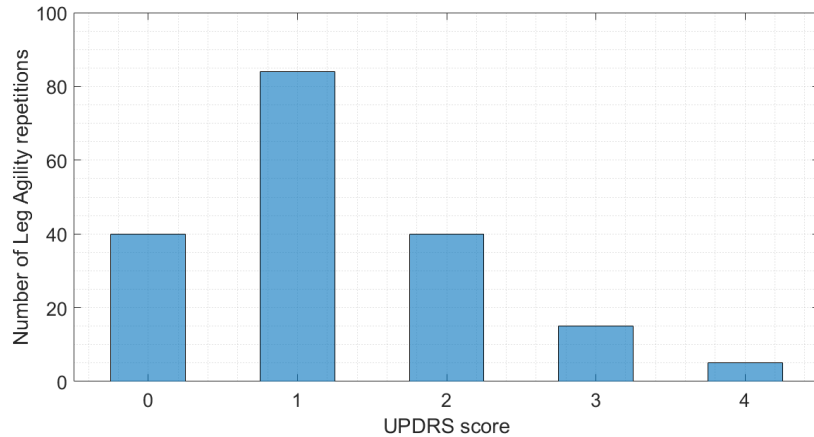


Figure 3.2: Distribution of the UPDRS scores assigned to the Leg Agility tasks.

3.4 Pre-processing

After the raw measurements were available in the desired format, some pre-processing was needed. According to Salarian et al [7], frequencies of 4-8 Hz are common for tremor (not investigated in this work), while intentional human movement seldom exceeds frequencies of 3.3 Hz. Therefore, a Chebyshev Type I lowpass filter with a frequency of 3.5 Hz was used to filter the measurement data with help of Matlab's `filtfilt` function before features were calculated. The stopband attenuation is of 20 dB at 4 Hz. The effect of this filter on the measurements is shown in Fig 3.3.

3.5 Defined features

A number of features were chosen based on knowledge about motion movements in Parkinson's disease and the experimental set-up, but also on insights provided by the literature on other similar studies [2, 8, 9, 10, 11]. Table 3.2 shows a list of the considered features, while from subsection 3.5.1 to 3.5.11 a detailed description of each single feature is exposed.

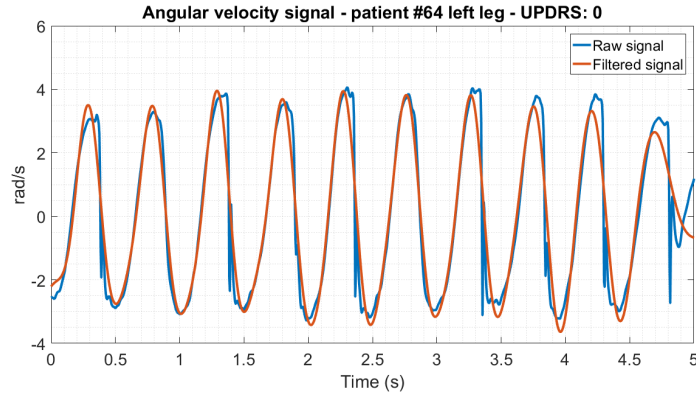


Figure 3.3: Raw and bandpass filtered gyroscope measurements of the left leg of patient 64.

Table 3.2: List of features used in this thesis work.

Feature	Description
n.1	Number of movements
n.2	Mean time interval between movements
n.3	STD of the time intervals
n.4	Thigh inclination trend
n.5	Mean peak value
n.6	Max peak value
n.7	RMS of angular velocity signal
n.8	Range of angular velocity signal
n.9	Max angular velocity value
n.10	Entropy of angular velocity signal
n.11	Dominant frequency
n.12	Ratio of dominant frequency power to total
n.13	RMS of acceleration signal
n.14	Range of acceleration signal
n.15	Max acceleration value
n.16	Entropy of acceleration signal

3.5.1 Number of movements

The number of leg movements, defined as peaks in the pitch signal, have been counted for each LA trial and used as one of the features. Since the MDS-UPDRS requests 10 repetitions, this feature can distinguish between patients who can accomplish the goal and those who cannot reach it. When extracting this feature, the MATLAB function `findpeaks` was used. Figure 3.4 shows the performance of the peak finding algorithm when it is applied on two patients affected by Parkinson’s disease with UPDRS 0 (a) and 3 (b).

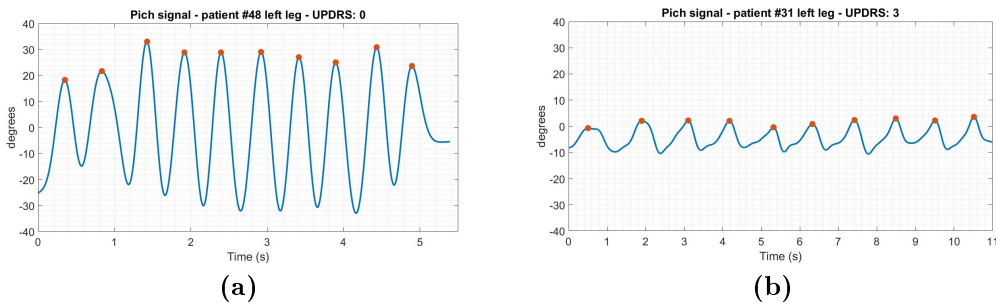


Figure 3.4: Peaks found by ready-made function `findpeaks`. Example of UPDRS 0 (a) and UPDRS 3 (b)

3.5.2 Mean time interval between movements

The i -th time interval $I(i)$ between consecutive thigh movements is defined as:

$$I(i) = t_P(i + 1) - t_P(i)$$

where $t_P(i+1)$ is the time associated with the peak of the $(i+1)$ -th repetition and $t_P(i)$ is the peak instant of the i -th repetition.

The feature used in this analysis is the mean time interval [dimension: (s)]:

$$I_{mean} = \frac{\sum_{i=1}^9 I(i)}{9}. \quad (3.1)$$

This feature is used since one of the common traits of bradykinesia is that a patient affected by Parkinson’s disease is expected to have a longer interval between the movements, since it might be hard to initiate the movement, as illustrated by Griffiths et al. [4].

3.5.3 Standard deviation of the time intervals

The following standard deviation of the previous feature is considered [dimension: (s)]:

$$I_{SD} = \sqrt{\frac{\sum_{i=1}^9 (I(i) - I)^2}{8}} \quad (3.2)$$

which quantifies how much the time intervals differ from their mean value. This is considered an important variable because some patients can perform very different LA repetitions, in terms of time difference between consecutive peaks, within the same task session.

A high value of I_{SD} is a synonym for a large variability of the time interval values, while a low value stands for a vector of time intervals very close to each other. The latter case is expected for healthy people, the former one for PD patients.

3.5.4 Thigh inclination trend

Another feature that measures the endurance of the LA task is the evolution of the peak amplitudes over time, i.e. the trend of the thigh inclination from the beginning to the end of the LA session. In particular the feature considered here is the percentage decrease of the peak amplitude from the first five movements to the last five. This feature might be useful since healthy subjects are expected to have a greater endurance and lesser decrease in performing the task. A high value would be synonym for a severe fatigue maintaining a constant maximum inclination. Fig. 3.5 shows an example of a Leg Agility repetition of a patient which was not able to maintain wide movements during the task.

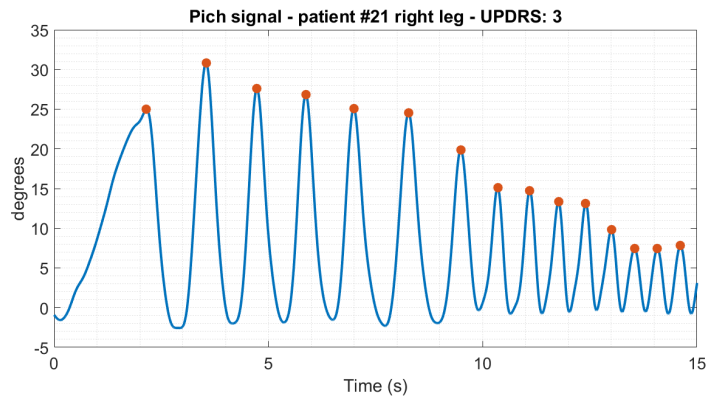


Figure 3.5: Pitch signal from a patient showing a clear decrement in amplitude.

3.5.5 Mean and max value of thigh inclination

Considering the peaks in the pitch signals, their maximum and mean value are calculated. These features are used since one of the common treats of PD patients that show bradykinesia symptom is the inability to make wide movements. It is expected the patients whose leg movements were rated as 0 by the expert neurologists show wider thigh movements (i.e. larger value of the inclination signal) than those who are more affected by the symptom.

3.5.6 Maximum acceleration and angular velocity

Since the slowness of the execution of movements should be reflected by the measured angular velocities and accelerations, their maximum absolute value is taken into account. Griffith et al. [4] have shown in their work the usefulness of the greatest acceleration as a predictor (feature). The value is given by:

$$x_{max} = \max (|x[n]|) \quad (3.3)$$

where $n = 1, 2, \dots, N$ is the sample index and x is the acceleration of the movements or the angular velocity (for x-axis, y-axis and z-axis).

3.5.7 Range of acceleration and angular velocity

This feature might be of interest for the assessment of bradykinesia, since theoretically the range should be smaller for patients suffering from bradykinesia due to smaller movements with respect to healthy subjects. The range is defined as:

$$r_x = \max (x[n]) - \min(x[n]) \quad (3.4)$$

where $n = 1, 2, \dots, N$ is the sample index and x is the acceleration of the movements or the angular velocity. In this work the z-axis acceleration and the x-axis angular velocity are taken into account.

3.5.8 Root Mean Square value

The RMS have been also used for accelerometer signals by Cancela et al. [3] and for gyroscope signals by Salarian et al. [7]. In statistics, the Root Mean Square (RMS) value of a signal is given by:

$$x_{RMS} = \sqrt{\frac{1}{N} \sum_{n=1}^N x^2[n]} \quad (3.5)$$

where $n = 1, 2, \dots, N$ is the sample index and x is the acceleration of the movements or the angular velocity.

3.5.9 Signal Entropy

Signal entropy is a measure of the uncertainty associated with the signal. This predictor was used for the quantification of bradykinesia, dyskinesia and tremor with help of accelerometer measurements by Patel et al [8]. It also shows strong distinctions for dyskinesic movements [49]. Signal spectral entropy (defined by Shannon) is calculated as:

$$H = - \sum_{m=1}^N P(m) \log_2 P(m) \quad (3.6)$$

where $P(m)$ is the probability distribution.

3.5.10 Dominant Frequency Component

To extract features from the frequency domain some frequency analysis is required. The aim is to present the signal in the frequency domain by estimating its power spectral density (PSD). The PSD estimation can be based on a Fourier transform or Wavelet transform or on parametric modeling of the signal.

In this thesis, the Fourier-based approach has been used for analysis. The Discrete Fourier Transform (DFT) of a discrete signal x is defined by:

$$X[k] = \sum_{n=0}^{N-1} x[n] e^{-j \frac{2\pi kn}{N}}. \quad (3.7)$$

where N is the total number of samples of the signal. In this case $x[n]$ is the signal derived from both the accelerometer and the gyroscope.

There are different PSD estimators available. In this thesis work, periodograms (i.e. direct method for PSD estimation) have been used for analysis.

The variance of the periodogram estimation can be reduced by averaging the periodograms over short signal epochs. Windowing (i.e. multiplying the signal with a window function) is often used for decreasing the spectral leakage. In Welch's periodogram approach, discrete window function is applied to each signal epoch and the sub-series are allowed to overlap (50% overlapping has been used here). The built-in MATLAB function `pwelch` has been used.

The dominant frequency f_{dom} is the frequency for which the PSD $P(f)$ is maximal. The dominant frequency component has been also used as a predictor by Patel et al. [8] and Bonato et al. [2] for accelerometer measurements.

3.5.11 Ratio of dominant frequency power to total power

The ratio of the dominant frequency power to total power (computed considering the PSD) was used as a feature by Patel et. al. [8] when studying classification of different motor symptoms based on accelerometer data. They found that this kind of feature was one especially suitable to capture signal characteristics from both tremor, dyskinesia and bradykinesia [8].

3.6 Machine learning algorithms

Machine learning (ML) is an application of artificial intelligence (AI) that automatically detects meaningful patterns in data and gives computers the ability to "learn" and improve from experience [50]. Machine learning has driven advances in many areas, from computer vision to automatic speech recognition. Its ability to extract information from data makes research in machine learning for medicine determining [51]. In fact, healthcare is a natural arena for the application of machine learning, especially as sensors provide large amounts of data to answer clinical questions.

Machine learning is capable of offering automatic learning techniques in biomedical signal and image processing, disease diagnosis, brain-computer interfaces, clinical interpretation and analysis, cardiovascular mechanics, drug development and robotic surgery [52].

Two of the most widely adopted machine learning methods are:

- **Supervised learning** which is based on example input data that is labeled. In other words, this kind of algorithm uses a ground truth (i.e. there is a prior knowledge of what the output values should be). The aim of supervised learning is to find a function which best approximates the relationship between input and output. It is called supervised because the learning process can be thought of as a teacher supervising the procedure [53].
- **Unsupervised learning** which provides the algorithm with no labeled data in order to allow it to find patterns or inherent structure within its input data. Unlike supervised learning, there are neither correct answers nor a teacher [53].

In this work supervised learning method has been used. Data has been labeled by the expert neurologists as UPDRS 0-1-2-3-4.

In the machine learning field, there is no algorithm that works best for every problem, especially for supervised learning. There are many factors at play (size of dataset, structure, number of features, etc). For example, decision trees are robust to outliers, can learn non-linear relationships and work for both categorical and continuous variables, but they are prone to overfitting. Deep neural networks perform very well on audio, image and text data, but often require a large amount of data and their training needs huge computational complexity [54]. Support Vector Machines methods can model non-linear decision boundaries and are robust against overfitting, but they

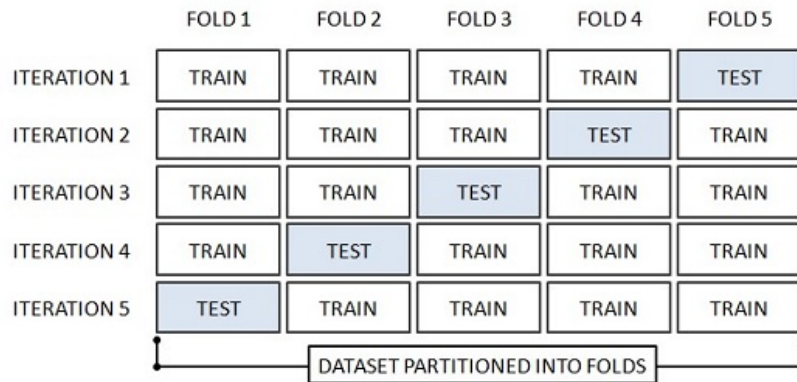


Figure 3.6: Illustration of the procedure of cross-validation. For each iteration, one fold is left out and used as a test set, while the other folds are used combined as a training set.

are memory intensive. K-Nearest Neighbor algorithms are computationally expensive and can be slow in the predicting phase [55].

3.6.1 Training and validation of methods

There are different approaches used in machine learning to evaluate the trained model and its performance. When a very large amount of observations are available, it may be feasible to divide the original data set into a training set and a test set prior to model development. The model is initially fit on a training set, that is a set of examples used to fit the parameters of the model. Then, the obtained model can be used to predict the response of each of the test set observations. However, since the dataset available in this work is quite limited, a cross-validation approach is used.

The k -fold cross-validation approach is based on dividing the dataset into k number of folds with roughly the same size. Then $k - 1$ folds are used as a training set and the last fold is used as a test set. Figure 3.6 displays the procedure of cross-validation and how one fold is left out for each iteration and used as a test set. The advantage of this method over repeated random sub-sampling is that all observations are used for both training and validation, and each observation is used for validation exactly once. In particular, when $k = n$ (with n being the number of observations), the k -fold cross-validation is exactly the leave-one-out cross-validation. That means that n separate times, the model is trained on all the data except for one point and a prediction is made for that point (where, here, a point means a Leg Agility repetition).

3.6.2 k-Nearest Neighbor (kNN)

kNN is a very popular classification technique due to its simple specification. It classifies unlabeled examples based on their similarity to the instances of the training set (or labeled vectors of features) [56]. It is a *non parametric* learning algorithm that assumes that the available data is in the so-called *feature space*, so that the data points have the notion of distance. It is a *non parametric* algorithm since it does not make any assumptions on the data distribution.

The kNN procedure for classifying a point (i.e. a measurement) to one of n classes involves these steps:

- Determine the k nearest points of the training set to the new measurement to be classified, using an appropriate distance metric;
- Assigning the new measurement to the class with most representatives within the k nearest neighbor.

In other words, the very intuitive idea of kNN is the following: if most adjacent vectors of a test sample in a feature space belong to one certain class, this sample most likely is part of this category [57].

This classification algorithm is very simple since the only requirements are the number of neighbors k , the distance metric and the training dataset. Its limitations are the large storage requirements and the computational expensiveness [57].

If $k = 1$ the class is assigned to the test sample considering only its nearest neighbor in the training set. As a general rule, a large value of k extends the neighborhood to the domain of other categories, while a small value can imply a sensitivity to noise. For this reason k is selected as a trade-off between them [56]

Fig 3.7 shows an intuitive example of kNN classification technique. In a 2-D plane, the green square is the sample to be classified and the two possible classes are the red stars and the blue triangles. It is obvious that, if the number k of neighbors is set to 5, the point is classified to the blue triangles. It is considered to be part of the red stars if the k is set to 10.

The model for kNN algorithm has been built in MATLAB using the function `fitcknn`. The function `predict` has been implemented to test and predict the UPDRS values.

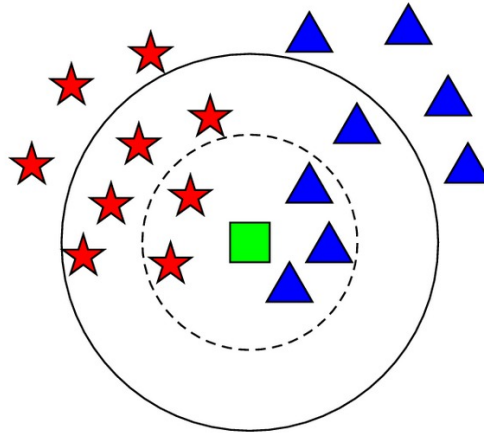


Figure 3.7: Basic principle of kNN classification method. From [57]

3.6.3 Support Vector Machine (SVM)

Support Vector Machine is a supervised learning method and one of the best techniques used in Machine Learning tasks. It was initially designed for binary classification (i.e. with the purpose of separating two classes), but it can be used also for multiclass problems. The objective of the SVM algorithm is to:

- Project via a certain kernel function the training samples (called *input space*) in a higher-dimensional space (called *feature space*) where the objects belonging to the two different classes are linearly separable [58];
- Constructs a hyperplane that maximizes the separation between the two classes of points, being the separation margin measured by l_2 -norm [59].

In Fig 3.8 two linearly separable sets of data with a separating hyperplane (the thick line) are depicted, as an example. The purpose of the hyperplane is to leave the closest points (i.e. those which form the margin, called "support vectors") at maximum distance [56].

The classical approach for multiclass classification is to combine several binary SVM classifiers, each of which solves a sub-problem of the original multi-class classification problem. One of the implementation of multiclass SVM classification is the so-called *one-vs-all* method. It consists of n SVM models where n is the number of classes. Each binary classifier is responsible for distinguishing one of the classes from all other classes [58]. The i -th model considers all of the examples in the i -th class with positive labels, and all

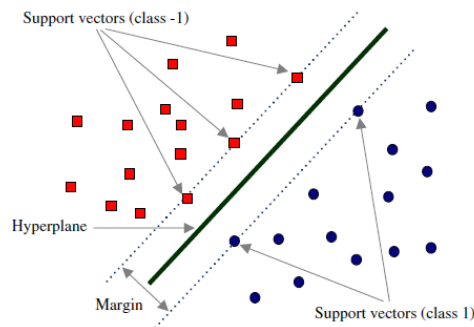


Figure 3.8: Two linearly separable datasets with the hyperplane which maximizes the distance between the two groups of data. From [60]

the others with negative labels. In the validation process, the classifier that gives a positive output indicates the output class.

Another method is called *one-against-one* and constructs $n(n-1)/2$ binary classifiers with considered data from two classes, on which it is trained. Each binary classifier is responsible for distinguishing between a different pair of classes [58]. The learning phase is performed using as training data only the original data set that contains samples of the two considered class labels, whereas the other class instances are ignored [56]

The MATLAB functions `templateSVM` and `fiscoc` were used to get a SVM learner template and build the model. The prediction was done using the function `predict`.

3.6.4 Neural networks (NN)

An artificial Neural Network (NN) is a computational system inspired by the way the human brain works. It consists of simple processing units, the neurons, and weighted connections between them. Each neuron has weighted inputs, an activation function and one output. The inputs are multiplied by the weights, then they are summed and passed through the function which produces the output for this neuron. Commonly used activation functions are the sigmoid, the linear and the tanh functions [61].

The general structure of a NN is composed of an input layer, one or some hidden layers and an output layer. Fig. 3.9 shows a Neural Network architecture.

There are two main types of connections when describing an artificial network:

Feedback architecture. The network has connections from the output

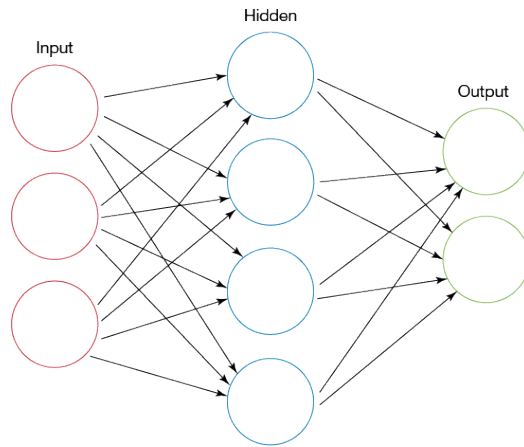


Figure 3.9: Artificial Neural Network architecture. From [62]

layer to the input neurons. Such a NN can keep a memory of the previous state so that the output in a state depends both on input signals and the previous states of the network [62];

Feedforward architecture. It is characterized by the absence of a feedback connection in the network, so that it cannot keep a record of the previous states (i.e. the previous output values).

One of the key elements of a NN is its ability to learn [61]: through the adjusting of weights it can change its internal structure based on the flow of information. Neural Network can be described as complex *adaptive* systems [63]. According to the back-propagation rule, the net is trained to map input data by iteratively adjusting the connection weights. The optimization of the weights is made by backward propagation of the error during training or learning phase of the algorithm. The objective is to reduce the difference between the output values and the target values.

While implementing a neural network, the input layer consists of a number of nodes equal to the number of features. The number of nodes to use for the hidden layer might vary, but it is standard to have a number between the number of nodes used in the output and the input layer [61]. The MATLAB function `feedforwardnet` implements a feedforward neural network. To initialize and train the network on a given training set, the function `init` and `train` were used.

concept of finding the way to maximize the class-separability [68]. LDA is also closely related to Principal Component Analysis (PCA) because they both look for linear combinations of variables which best explain the data. However LDA explicitly attempts to model the difference between the classes of the available data while PCA does not take into account any difference in class [69].

3.7 Hypothesis for feature set

Before implementing the methods on the available data, some hypotheses were made in order to determine if a certain kind of features or sensors affected the performance more than others.

3.7.1 Hypothesis 1: All available features

The first hypothesis is to use all the available features, generated according to the described procedure in Section 3.5. This means that features generated from both the accelerometer and the gyroscope data were used.

3.7.2 Hypothesis 2: Features from accelerometer

To further explore the effect of the accelerometer data, the second hypothesis uses the signals acquired from the accelerometer.

3.7.3 Hypothesis 3: Features from gyroscope

The last hypothesis uses all the features gathered from the gyroscope signals.

3.8 Statistical and performance descriptors

3.8.1 Boxplot

A boxplot (or a *box and whisker diagram*) is a standardized way of representing the distribution of data using five number summary: minimum, first quartile, median value, third quartile, maximum. Fig. 3.11 represents the structure of a boxplot.

The line splitting the box in half is the median of the values. Half of the cases have a value greater than the median, and half have a value lower. The median value is chosen since, unlike the mean value, is less influenced by extreme values.

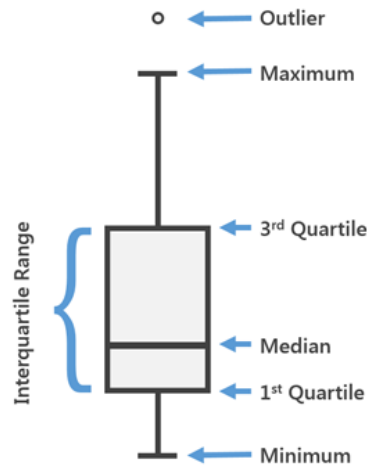


Figure 3.11: A boxplot with its terminology.

The bottom of the box represents the 1st quartile (or 25th percentile), while the top of the box indicates the 3rd quartile (or 75th percentile). It means that 25% of cases have values below the 1st quartile and 25% of them have values above the 3rd quartile. This means that 50% of the case are represented within the box, also known as the interquartile range, or IQR. A large IQR indicates a large spread in values, while a smaller one shows that most values fall near the median [70].

The T-bars out of the boxes are called *inner fences* or *whiskers* and indicates the maximum and minimum values. Box plots optionally illustrate outliers as points extending beyond the whiskers. Outliers are extreme values (more than three times the height of the boxes).

3.8.2 Confusion Matrix

In predictive analytics, a confusion matrix is a table used as a descriptor of the performance of a classification model on a given test data for which the true values are known. It is a square matrix in which the rows represents the actual class and the columns the predicted one [71].

If we consider a simple binary classification, the confusion matrix is a table with two rows and two columns that reports the *false positives*, *false negatives*, *true positives*, and *true negatives*. Fig. 3.12 shows an example of a confusion matrix for a binary classification problem, with the correct terminology to be used when describing it.

Some rates are often computed from a confusion matrix for a binary

		Predicted class	
		<i>P</i>	<i>N</i>
Actual Class	<i>P</i>	True Positives (TP)	False Negatives (FN)
	<i>N</i>	False Positives (FP)	True Negatives (TN)

Figure 3.12: A confusion matrix for a binary classifier and its terminology.

classifier:

- Accuracy = $\frac{TP+TN}{TP+TN+FP+FN}$
- Precision or Positive Predictive Value = $\frac{TP}{TP+FP}$
- Negative Predictive Value = $\frac{TN}{TN+FN}$
- Sensitivity or True Positive Rate = $\frac{TP}{TP+FN}$
- Specificity or True Negative Rate = $\frac{TN}{TN+FP}$

Fig. 3.13 shows an example of confusion matrix for multiple classes. Each column represents the results of prediction for the corresponding class, while each row represents the actual class. The diagonal cells show the number (or the percentage) of correct classifications by the trained classifier, while the off diagonal cells represent the misclassified predictions.

		Prediction				
		Class 1	Class 2	Class 3	...	Class n
Actual	Class 1	Accurate				
	Class 2		Accurate			
	Class 3			Accurate		
	...				Accurate	
	Class n					Accurate

Figure 3.13: A confusion matrix for a multiclass classification problem.

Chapter 4

Results

In this chapter the results obtained in this thesis work are presented. In section 4.1 some plots showing angular velocity signals are described, while in section 4.2 some accelerometer measurements are shown. Section 4.3 illustrates some promising results in term of boxplots considering some of the available features. From section 4.4 to 4.6 the results obtained from the classification models are shown using the confusion matrices. Finally, section 4.7 presents the results from the binary classification, where UPDRS 0, 1 and 2 are grouped as a single class while UPDRS 3 and 4 form another class, with the aim of understanding if also a binary classification between the "slight" case and "severe" one is feasible.

4.1 Examples of angular velocity signals

The severity of the motor symptom (in this case, lower limb bradykinesia) is reflected on the angular velocity signal around the x-axis, i.e. the direction perpendicular to the femur in the coronal plane. Figure 4.1 illustrates how this signal changes from a normal condition (UPDRS 0 = no motor problems) to a severe situation (UPDRS 4 = the patient can only barely perform the task). It is clearly evident that both amplitude and regularity decrease along with the severity of bradykinesia. All the plots have the same y-axis in order to be able to visually compare the mentioned differences. It is also useful to notice how the time interval needed to perform at least ten repetitions increases from UPDRS 0 to UPDRS 4 (from about 6 s to more than 15 s).

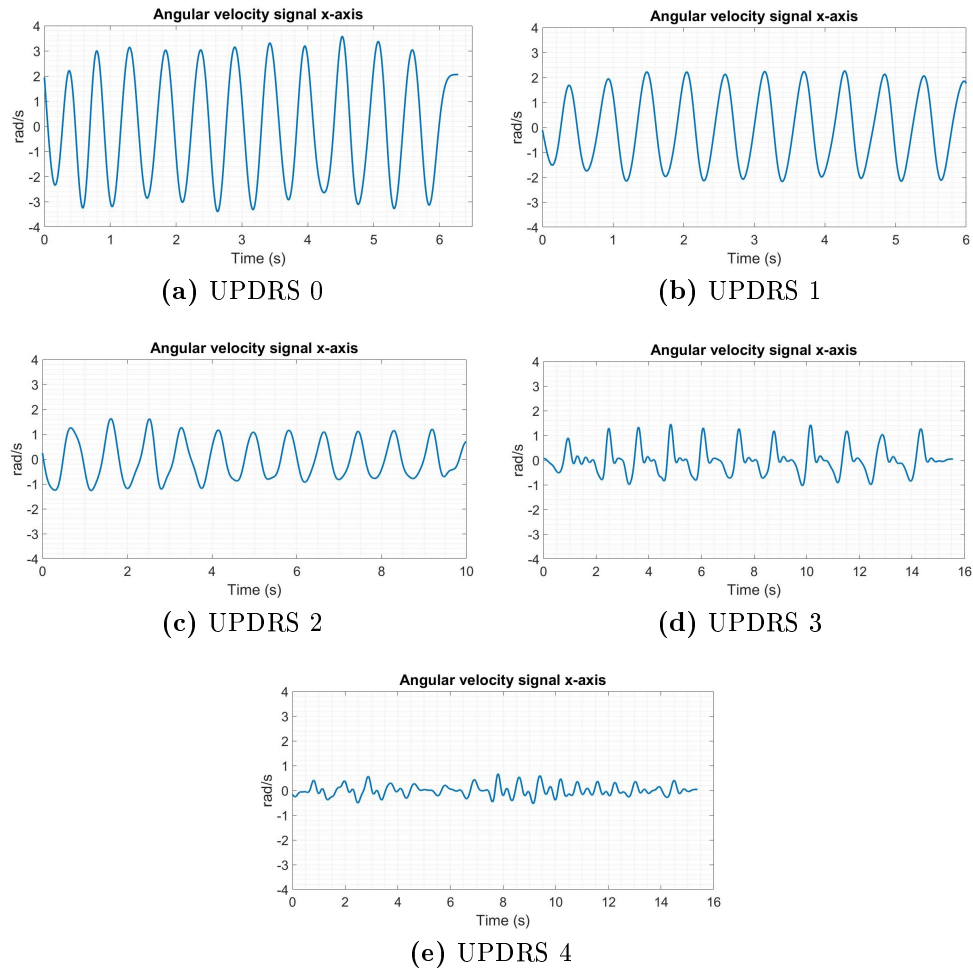


Figure 4.1: Time trajectories of x-axis angular velocity from UPDRS 0 to 4.

4.2 Examples of accelerometer signals

The same trend can be seen considering the accelerometer signals, shown in Fig 4.2. The amplitude decreases very much along with the severity of the considered motor symptom. The peaks detection in the condition of UPDRS 4 can be barely performed.

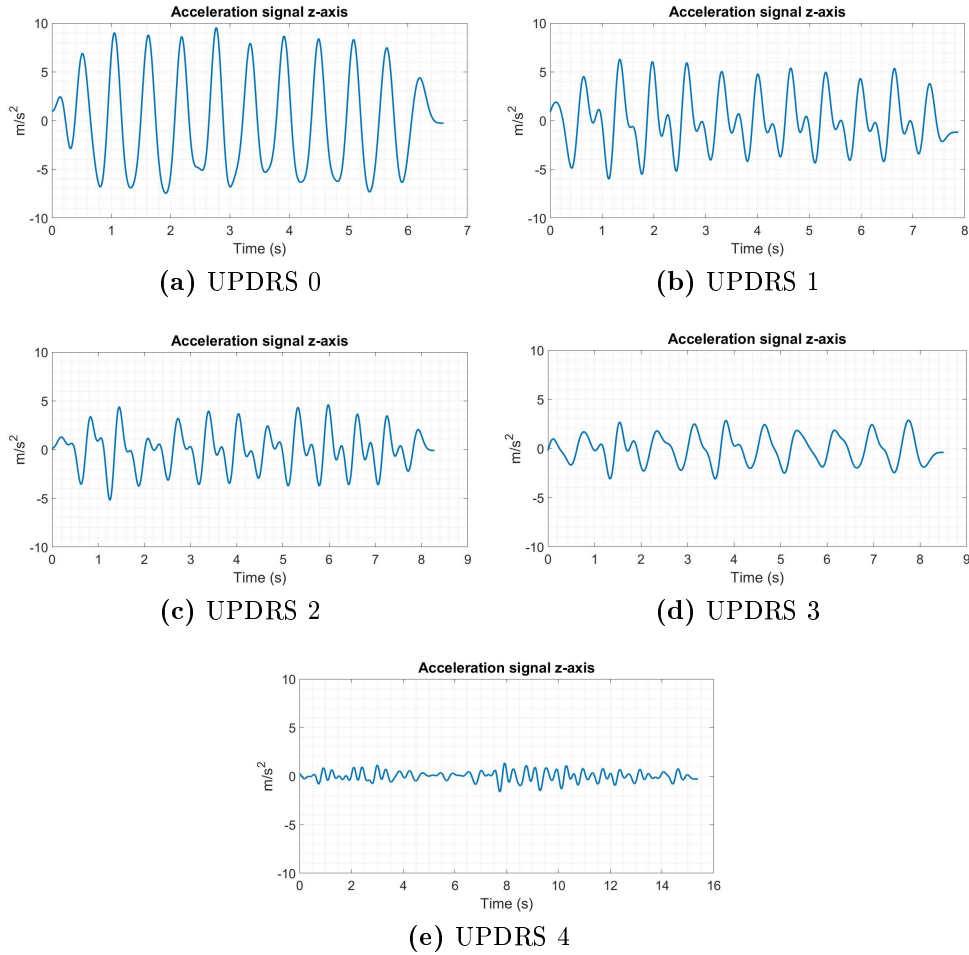


Figure 4.2: Time trajectories of z-axis acceleration from UPDRS 0 to 4.

4.3 Boxplots

In this subsection some boxplots of the most relevant features are considered.

Fig. 4.3 shows the boxplots for two acceleration-based features: the maximum value and the range of the signal. Both of them present a clear decreasing trend along with the severity of the bradykinesia symptom.

Fig. 4.4 shows the boxplots of the same previous features for the gyroscope signal (x-axis angular velocity). Like the acceleration case, one can notice a decreasing trend from UPDRS 0 (no problems) to UPDRS 4 (the severe case).

Fig. 4.5a presents only UPDRS 0-3 due to the fact that the Leg Agility

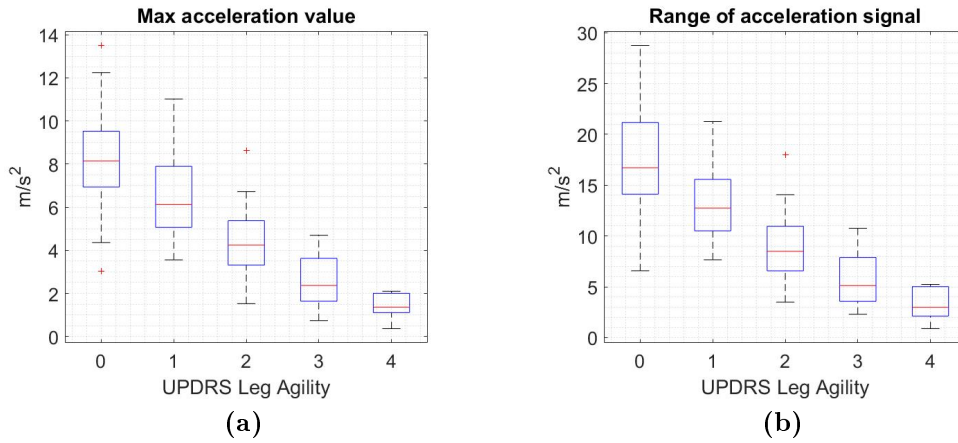


Figure 4.3: Boxplot showing a trend of both the maximum acceleration value (a) and the range of the signal values (b) along with the severity of the symptom.

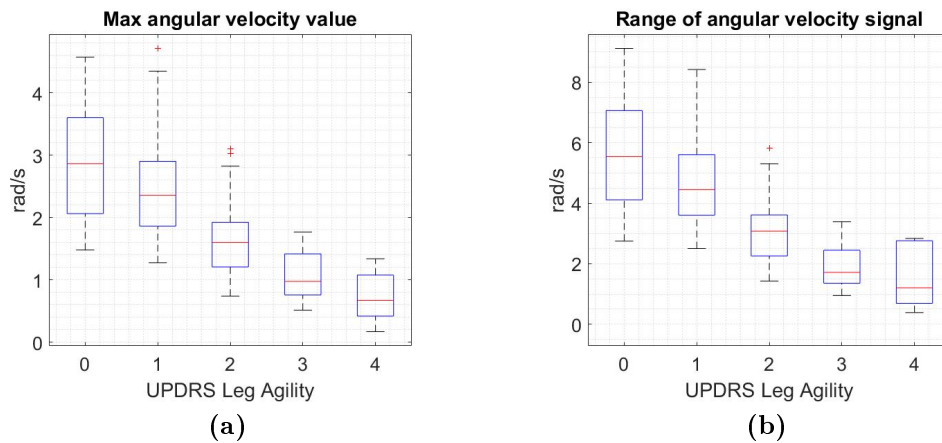


Figure 4.4: Boxplot showing a trend of both the maximum angular velocity value (a) and the range of the signal values (b) along with the severity of the symptom.

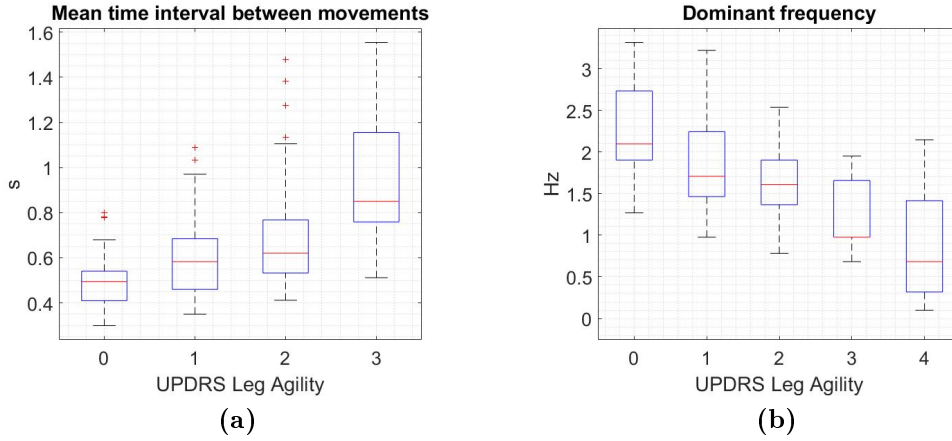


Figure 4.5: Boxplot of the mean time interval between movements (a) and the dominant frequency (b).

cases labeled as UPDRS 4 did not have real leg movements and, as a consequence, the mean time interval between movements could not be calculated.

4.4 Hypothesis 1: All available features

For this hypothesis all the available features (i.e. from orientation sensor, gyroscope and accelerometer) are considered. Table 4.1 illustrates the general performance of each classification models described in section 3.6, while the confusion matrices are given in Fig. 4.6, 4.7, 4.8.

Table 4.1: Correct classification percentage of the selected classification methods for each UPDRS class and overall performance. The best results come from Neural Networks (gray line).

Method	UPDRS 0	UPDRS 1	UPDRS 2	UPDRS 3	UPDRS 4	Overall
SVM linear	42.5 %	77.4 %	52.5 %	46.7 %	40 %	60.9 %
kNN (k=5)	40 %	79.8 %	50 %	46.7 %	40 %	60.9 %
kNN (k=10)	45 %	90.5 %	40 %	40 %	0 %	63 %
Neural Networks	75 %	81 %	65 %	86.7 %	60 %	76.1 %
L.D. Analysis	62.5 %	46.4 %	52.5 %	66.7 %	60 %	53.3 %
Decision Tree	37.5 %	75 %	37.5 %	60 %	0 %	55.4 %

Linear SVM - Confusion Matrix

True UPDRS	0	17 9.2%	23 12.5%	0 0.0%	0 0.0%	0 0.0%	42.5% 57.5%
	1	9 4.9%	65 35.3%	10 5.4%	0 0.0%	0 0.0%	77.4% 22.6%
	2	0 0.0%	17 9.2%	21 11.4%	2 1.1%	0 0.0%	52.5% 47.5%
	3	0 0.0%	0 0.0%	8 4.3%	7 3.8%	0 0.0%	46.7% 53.3%
	4	0 0.0%	0 0.0%	0 0.0%	3 1.6%	2 1.1%	40.0% 60.0%
			65.4% 34.6%	61.9% 38.1%	53.8% 46.2%	58.3% 41.7%	100% 0.0%
		0	1	2	3	4	
		Predicted UPDRS					

Figure 4.6: Confusion matrix based on the results from the Linear SVM classification model. The blue cell in the bottom right displays the overall correct classification percentage and incorrect classification percentage. The correctly classifies case are positioned diagonally (green) while the misclassifies cases are places in the other cells (red).

By examining Fig. 4.6 some important considerations have to be made. First of all, this SVM model classifies incorrectly only by one step on the UPDRS scale. One may also see that the main errors in classification was that true UPDRS 0 was incorrectly predicted as UPDRS 1 in 57.5 percent of the available signals, and the best classification was done for UPDRS 1, where 77.4 percent of the signals were correctly classified. For the whole multiclass classification, the Linear SVM model correctly classifies 60.9 percent of the available test observations.

Fig. 4.7 shows two confusion matrices when using the k-Nearest Neighbor classification model with $k = 5$ and $k = 10$. The overall performance is very similar to that of Linear SVM model (Figure 4.6) but in this case one UPDRS 4 has been classified as UPDRS 2 (figure (a)) and all the UPDRS 4 have been misclassified (figure (b)).

The confusion matrix in Fig. 4.8 displays a total classification percentage of 53.3 percent correctly classified observations. Although the lower total performance percentage, one can notice that with Linear Discriminant Analysis a good performance is obtained with the classification of UPDRS 0. In fact 62.5 percent of UPDRS 0 has been correctly classified, while the pre-

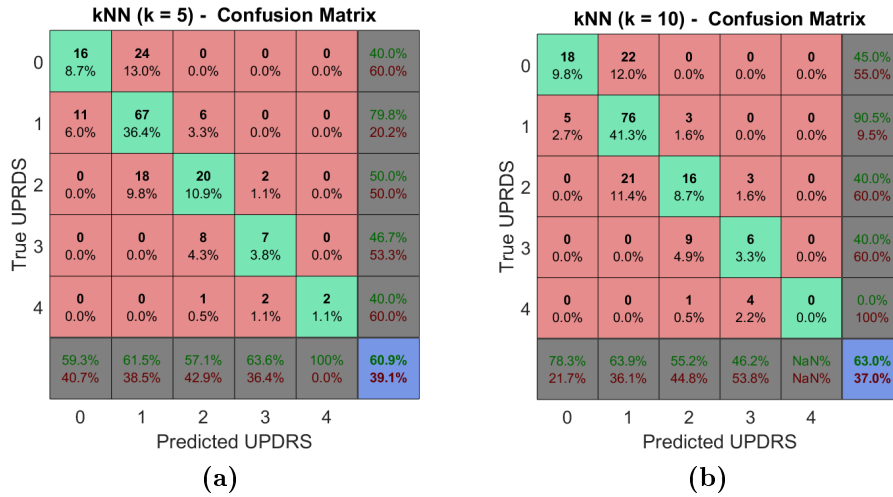


Figure 4.7: Confusion matrices based on the results from the kNN classification model.

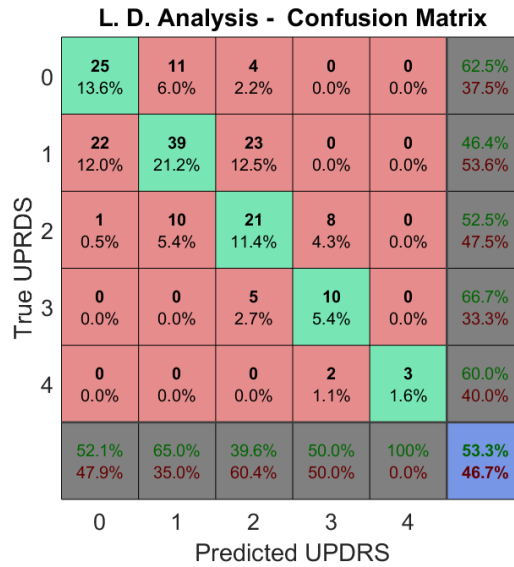


Figure 4.8: Confusion matrix based on the results from the Linear Discriminant Analysis (LDA) model.

vious models (kNN and SVM) were not able to distinguish between these two classes. The same observation can be made about the classification of UPDRS 4, where, alike the other classifiers, 60 percent of the cases has been correctly classified.

Decision Tree - Confusion Matrix

True UPDRS	0	15 8.2%	24 13.0%	1 0.5%	0 0.0%	0 0.0%	37.5% 62.5%
	1	13 7.1%	63 34.2%	6 3.3%	2 1.1%	0 0.0%	75.0% 25.0%
	2	1 0.5%	16 8.7%	15 8.2%	8 4.3%	0 0.0%	37.5% 62.5%
	3	0 0.0%	0 0.0%	5 2.7%	9 4.9%	1 0.5%	60.0% 40.0%
	4	0 0.0%	0 0.0%	0 0.0%	5 2.7%	0 0.0%	0.0% 100%
			51.7% 48.3%	61.2% 38.8%	55.6% 44.4%	37.5% 62.5%	0.0% 100%
		0	1	2	3	4	
		Predicted UPDRS					

Figure 4.9: Confusion matrix based on the results from the Decision Tree model.

By examining Fig. 4.9 it is evident that, when using the Decision Tree method, the five cases labeled as UPDRS 4 have not been distinguished from UPDRS 3. Also the correct classification percentage of UPDRS 0 is very low.

The result of Neural Network is presented in Fig. 4.10. Here 76.1 percent of the observations were correctly assigned to the right class and the performance is very good for all the five classes. The best classification cases, like all the other previous methods, was for observations with true UPDRS 1 and UPDRS 3. The errors are only by one step on the UPDRS scale. This model has two inner layers of 16 neurons, and the hyperbolic tangent sigmoid as transfer function (`tansig`).

4.5 Hypothesis 2: Features from accelerometer

In this section the results considering the use of only accelerometer-based features are presented.

Neural Network - Confusion Matrix

True UPDRS	0	30 16.3%	10 5.4%	0 0.0%	0 0.0%	0 0.0%	75.0% 25.0%
	1	14 7.6%	68 37.0%	2 1.1%	0 0.0%	0 0.0%	81.0% 19.0%
	2	0 0.0%	12 6.5%	26 14.1%	2 1.1%	0 0.0%	65.0% 35.0%
	3	0 0.0%	0 0.0%	2 1.1%	13 7.1%	0 0.0%	86.7% 13.3%
	4	0 0.0%	0 0.0%	0 0.0%	2 1.1%	3 1.6%	60.0% 40.0%
			68.2% 31.8%	75.6% 24.4%	86.7% 13.3%	76.5% 23.5%	100% 0.0%
		0	1	2	3	4	
		Predicted UPDRS					

Figure 4.10: Confusion matrix based on the results from the supervised Neural Network model for Hypothesis 1.

Linear SVM - only ACC - Confusion Matrix							kNN (k = 5) - only ACC - Confusion Matrix							
True UPDRS	0	11 6.0%	28 15.2%	1 0.5%	0 0.0%	0 0.0%	27.5% 72.5%	0	15 8.2%	23 12.5%	2 1.1%	0 0.0%	0 0.0%	37.5% 62.5%
	1	13 7.1%	64 34.8%	7 3.8%	0 0.0%	0 0.0%	76.2% 23.8%	10 5.4%	70 38.0%	4 2.2%	0 0.0%	0 0.0%	83.3% 16.7%	
	2	0 0.0%	16 8.7%	19 10.3%	5 2.7%	0 0.0%	47.5% 52.5%	0 0.0%	17 9.2%	19 10.3%	4 2.2%	0 0.0%	47.5% 52.5%	
	3	0 0.0%	0 0.0%	7 3.8%	8 4.3%	0 0.0%	53.3% 46.7%	0 0.0%	0 0.0%	11 6.0%	4 2.2%	0 0.0%	26.7% 73.3%	
	4	0 0.0%	0 0.0%	1 0.5%	4 2.2%	0 0.0%	0.0% 100%	0 0.0%	0 0.0%	1 0.5%	4 2.2%	0 0.0%	0.0% 100%	
			45.8% 54.2%	59.3% 40.7%	54.3% 45.7%	47.1% 52.9%	NaN% NaN%	55.4% 44.6%	60.0% 40.0%	63.6% 36.4%	51.4% 48.6%	33.3% 66.7%	NaN% NaN%	58.7% 41.3%
		0	1	2	3	4		0	1	2	3	4		
		Predicted UPDRS						Predicted UPDRS						

(a) (b)

Figure 4.11: Confusion matrices based on the results from the SVM (a) and kNN (b) classification models for Hypothesis 2.

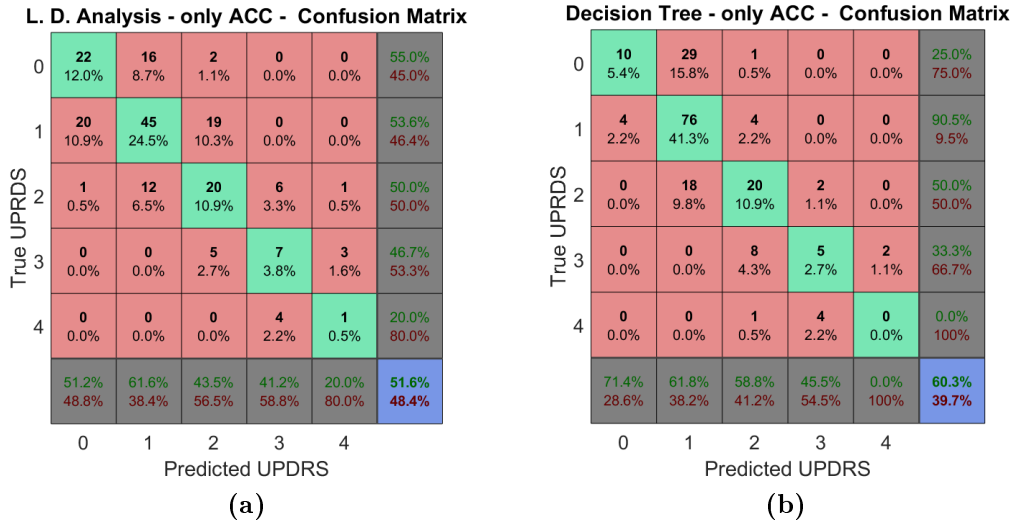


Figure 4.12: Confusion matrices based on the results from the Linear Discriminant Analysis (a) and Decision Tree (b) classification models for Hypothesis 2.

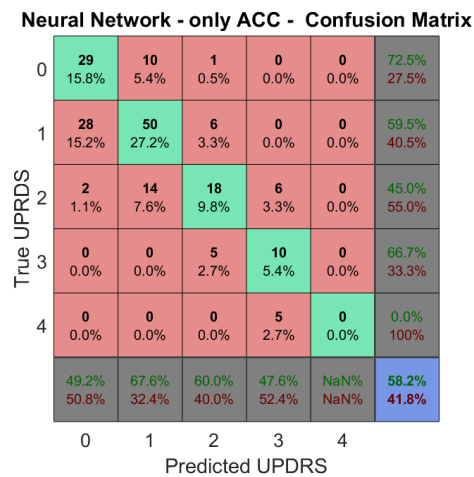


Figure 4.13: Confusion matrix based on the results from the supervised Neural Network model for Hypothesis 2.

4.6 Hypothesis 3: Features from gyroscope

In this section the results considering the use of the gyroscope-based features are presented.

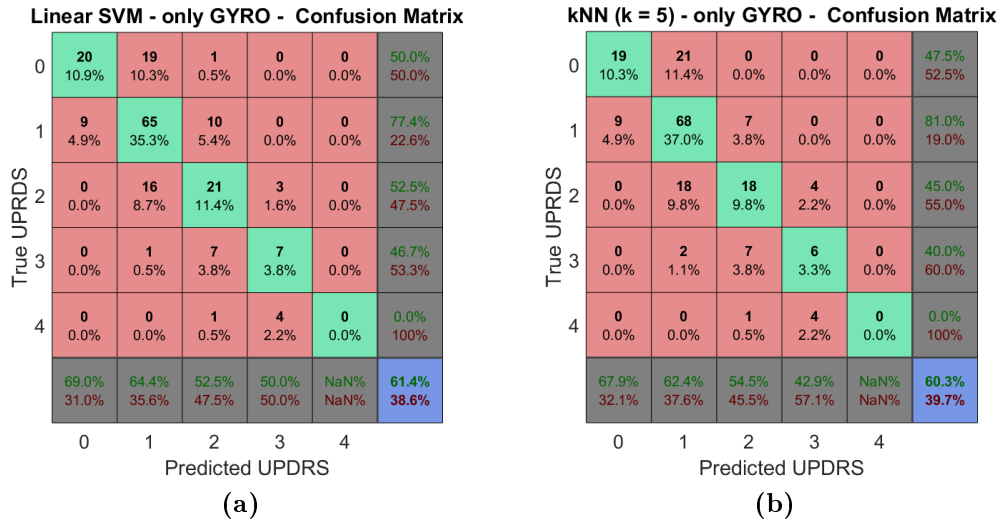


Figure 4.14: Confusion matrices based on the results from the SVM (a) and kNN (b) classification models for Hypothesis 3.

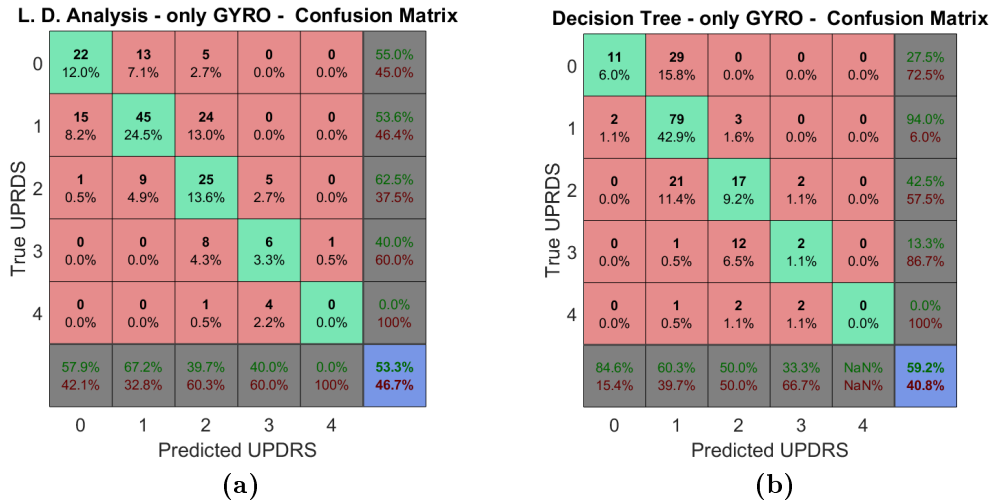


Figure 4.15: Confusion matrices based on the results from the Linear Discriminant Analysis (a) and Decision Tree (b) classification models for Hypothesis 3.

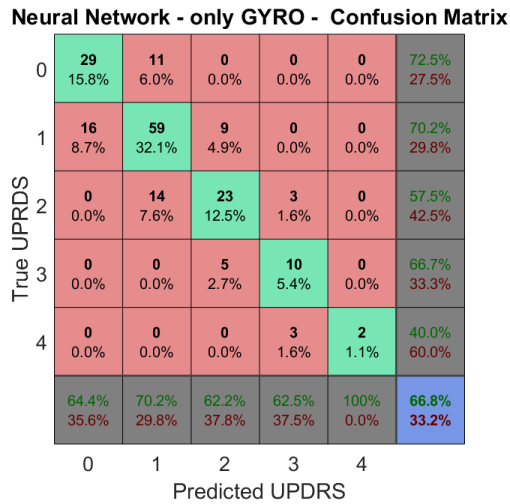


Figure 4.16: Confusion matrix based on the results from the supervised Neural Network model for Hypothesis 3.

4.7 Binary classification

It is also interesting to have a classification model able to distinguish between a slight and a severe motor condition. For this reason, in this section all the data from UPDRS 0 and 1 are now considered as the "slight" group, while the cases from UPDRS 2, 3 and 4 as the "severe" group. In the following figures some results from the main classification models (kNN, SVM and Neural Network) for the binary case are presented.

Neural Network (Binary) - Confusion Matrix

True Slight	121 65.8%	3 1.6%	97.6% 2.4%
	10 5.4%	50 27.2%	83.3% 16.7%
True Severe	92.4% 7.6%	94.3% 5.7%	92.9% 7.1%
	Predicted Slight	Predicted Severe	

Figure 4.17: Confusion matrix based on the results from the supervised Neural Network model.

For the binary classification problem a great performance is achieved by almost all the presented classification methods. In particular, with the Neural Network technique an overall percentage of correct classification of 92.9 percent is reached.

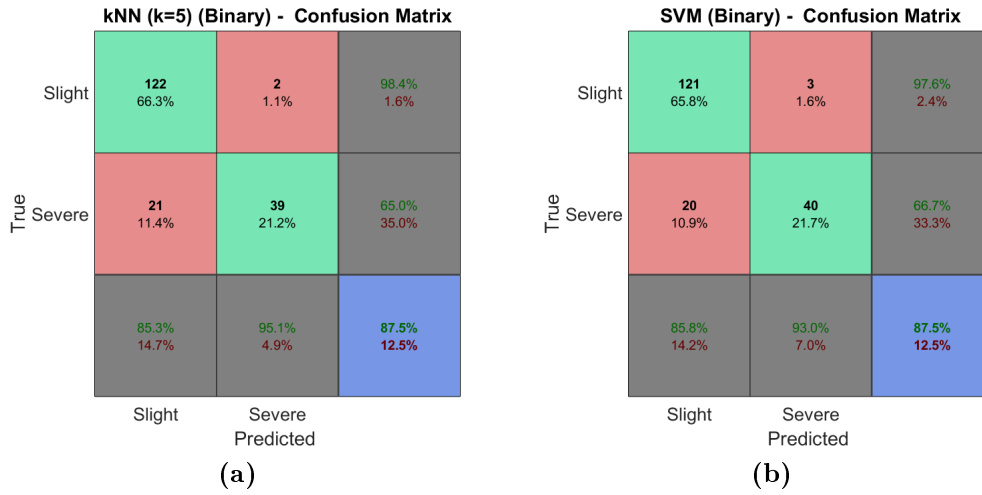


Figure 4.18: Confusion matrices based on the results from the kNN (a) and SVM (b) classification models.

4.8 Control population results

Table 4.2: Classification of control population signals.

Patient	UPDRS	
	Leg Agility RIGHT	Leg Agility LEFT
CTRL 1	1	1
CTRL 2	2	1
CTRL 3	1	1
CTRL 4	1	1
CTRL 5	1	1
CTRL 6	1	1
CTRL 7	1	1
CTRL 8	1	1
CTRL 9	1	1
CTRL 10	1	1

Chapter 5

Discussion

This work has investigated the capability of some machine learning algorithms to quantify and classify signals acquired from Parkinson's disease patients.

By looking at the boxplots presented in Chapter 4, it is important to highlight the clear decreasing trend of some features along with the severity of the motor symptom of bradykinesia. The maximum value and the range of both the acceleration and gyroscope signals turned out to be significant features for the assessment of bradykinesia. The mean time interval between consecutive movements (valid for UPDRS 0-1-2-3) shows an increasing behaviour from the case of UPDRS 0 to that of UPDRS 3. This was imaginable since the neurologist rates the severity by looking at the leg movements: the wider two consecutive movements are, the greater will be the UPDRS score. The dominant frequency proved to be related to the severity of the motor symptom: for UPDRS 0-1-2 it is greater because it is synonym for faster movement, while it decrements for the more severe cases (UPDRS 3-4).

From the confusion matrices presented in Chapter 4, one may observe that it is more common that the models classify incorrectly by one step on the UPDRS scale, rather than, for example, assigning a case with UPDRS 0 to class 3. This is an excellent result because in the clinical practice the neurologists can disagree about the score to be assigned, but usually by one step value.

The better overall correct classification percentages are reached by SVM model (Fig. 4.6) with 60.9 percent and Neural Network model (Fig. 4.10) with 76.1 percent. The most accurate classification was achieved for observations with true class 1 and 3. The kNN, Linear Discriminant Analysis and Decision Tree (Fig. 4.7, Fig. 4.8 and Fig. 4.9) show their inability to recognize the cases of UPDRS 4. Maybe with some fine-tuning and with more

training examples the accuracy of assising to this class can be improved.

The use of only accelerometer-based or gyroscope-based features has turn out to be not relevant. In a nutshell, the calssification performance improves when all the features are considered.

Concerning the binary classification problem, where UPDRS 0-1 forms one group and UPDRS 2-3-4 forms the other, has shown important results. A classification accuracy of up to 90 percent is reached with kNN, SVM and Neural Network techniques. The errors made in this case are the same of the multiclass classification: the cases in which UPDRS 1 have been classified as UPDRS 2 and vice versa.

The signals gathered from Control population have been classified as UPDRS 1 in almost all the cases. This means that a slight bradykinesia has been found in this population, probably due to the age of the partecipants (mean age: 87 years). Since the algorithm is not a Parkinson's disease diagnose system, it is obvious that some healthy people could be labeled as UPDRS 1 or even 2.

Chapter 6

Conclusion

The purpose of this thesis work was to investigate the possibility of using smartphone sensors for the acquisition of data and machine learning algorithms for the classification of the bradykinesia in Parkinson's disease. All data was collected from both gyroscope and accelerometer sensors, during a specific body movement in order to be able to classify the severity of the considered motor symptom.

In particular, in this thesis the use of a common smartphone is presented. It is a simple system that the patient can use in his/her domestic environment without any trouble and in which the leg movement is not hindered.

It should also be concluded that more training data is desirable, since the available dataset is not so large. In fact, the results for the classification between UPDRS 3 and 4 are not so accurate, but they are good enough to motivate further investigation. More signal examples from UPDRS 3 and 4 should be acquired to be able to better train the model on these classes.

This work has shown promising results regarding the ability to diagnose physical symptoms in Parkinson's disease patients using machine learning algorithms. The validity of these results is limited to the considered motion and to the quantification of bradykinesia, but similar considerations for different movements including motions of other body parts may prove interesting as well.

By having a patient with his/her smartphone located on the thigh, in the future physicians can be allowed to get a clearer view on symptom fluctuation during a patient's daily life. This continuous observation can help with the adjustment of medicine if it is tracked that the symptoms get more severe during certain times of the day. It would mean an increase in the quality of life of both the patients and their caregivers.

Appendix A

Parkinson's disease and Control population details

Table A.1: Parkinson's disease population recruited in this thesis work.

Patient ID	Age	Gender (M/F)	UPDRS Leg Agility RIGHT	UPDRS Leg Agility LEFT	Years from diagnosis
PD1	86	M	2	3	8
PD2	60	F	2	1	5
PD3	65	M	1	1	7
PD4	74	F	0	0	10
PD5	71	M	3	4	18
PD6	83	M	0	1	2
PD7	78	M	2	3	6
PD8	66	M	0	1	9
PD9	68	M	1	1	6
PD10	77	F	1	2	11
PD11	52	F	1	1	23
PD12	62	M	1	1	2
PD13	76	F	2	2	20
PD14	75	F	1	0	2
PD15	76	F	1	2	3
PD16	52	M	1	0	8
PD17	81	M	1	2	9
PD18	83	M	1	1	9
PD19	64	M	1	1	7
PD20	59	M	1	1	1
PD21	68	F	3	2	15

APPENDIX A. PARKINSON'S DISEASE AND CONTROL
POPULATION DETAILS

PD22	85	M	3	4	6
PD23	55	M	0	0	2
PD24	57	F	0	0	4
PD25	75	M	3	2	20
PD26	73	M	3	3	21
PD27	66	M	2	1	14
PD28	63	M	1	1	8
PD29	71	M	0	2	4
PD30	57	F	1	1	2
PD31	87	F	3	3	6
PD32	76	M	0	1	4
PD33	74	M	2	1	3
PD34	73	M	0	0	8
PD35	43	M	2	1	5
PD36	71	M	1	1	6
PD37	63	M	1	1	7
PD38	84	F	2	2	7
PD39	56	M	1	1	12
PD40	65	M	0	0	1
PD41	78	M	1	2	10
PD42	67	M	0	0	10
PD43	78	F	1	1	1
PD44	71	F	0	0	3
PD45	49	M	4	1	3
PD46	80	M	0	1	1
PD47	71	M	2	2	10
PD48	63	F	0	0	1
PD49	84	M	1	2	20
PD50	76	M	3	3	9
PD51	84	M	1	1	8
PD52	67	M	1	1	7
PD53	71	F	1	1	4
PD54	66	M	1	1	8
PD55	59	M	2	1	2
PD56	75	M	1	1	8
PD57	71	F	2	0	3
PD58	57	F	1	1	4
PD59	71	M	2	1	13
PD60	77	M	1	1	15
PD61	77	F	0	0	8
PD62	52	F	1	1	5

*APPENDIX A. PARKINSON'S DISEASE AND CONTROL
POPULATION DETAILS*

PD63	59	F	0	0	10
PD64	64	F	0	0	15
PD65	70	F	0	0	10
PD66	69	F	1	1	3
PD67	64	M	1	0	5
PD68	81	F	3	2	8
PD69	80	M	2	2	-
PD70	69	M	1	1	3
PD71	44	F	2	2	8
PD72	58	M	2	1	5
PD73	65	M	1	1	20
PD74	77	F	4	4	12
PD75	75	M	3	-	7
PD76	52	F	0	0	4
PD77	63	M	1	2	9
PD78	69	M	1	1	6
PD79	64	F	2	1	15
PD80	72	F	1	1	23
PD81	73	F	3	2	23
PD82	46	F	1	1	-
PD83	61	M	1	2	28
PD84	74	M	2	2	21
PD85	75	M	0	1	12
PD86	78	F	1	2	12
PD87	75	M	1	-	11
PD88	77	F	0	1	5
PD89	59	M	0	0	2
PD90	77	F	2	2	10
PD91	72	F	2	2	18
PD92	63	F	1	1	23
PD93	78	M	0	1	20

*APPENDIX A. PARKINSON'S DISEASE AND CONTROL
POPULATION DETAILS*

Table A.2: Control population recruited in this thesis work.

Patient ID	Age	Gender(M/F)
CTRL 1	88	F
CTRL 2	90	F
CTRL 3	98	M
CTRL 4	90	F
CTRL 5	86	F
CTRL 6	81	F
CTRL 7	88	F
CTRL 8	79	F
CTRL 9	88	M
CTRL 10	83	M

Bibliography

- [1] *La malattia di Parkinson*. 2011. URL: <https://http://www.parkinson-italia.it/parkinson/la-malattia>.
- [2] Paolo Bonato et al. “Data mining techniques to detect motor fluctuations in Parkinson’s disease”. In: *Engineering in Medicine and Biology Society, 2004. IEMBS’04. 26th Annual International Conference of the IEEE*. Vol. 2. IEEE. 2004, pp. 4766–4769.
- [3] J Cancela et al. “A comprehensive motor symptom monitoring and management system: The bradykinesia case”. In: *Engineering in Medicine and Biology Society (EMBC), 2010 Annual International Conference of the IEEE*. IEEE. 2010, pp. 1008–1011.
- [4] Robert I. Griffiths et al. “Automated assessment of bradykinesia and dyskinesia in Parkinson’s disease”. In: *Journal of Parkinson’s disease* 2.1 (2012), pp. 47–55.
- [5] Matteo Giuberti et al. “Assigning UPDRS scores in the leg agility task of Parkinsonians: Can it be done through BSN-based kinematic variables?” In: *IEEE Internet of Things Journal* 2.1 (2015), pp. 41–51.
- [6] Dustin A Heldman et al. “The modified bradykinesia rating scale for Parkinson’s disease: reliability and comparison with kinematic measures”. In: *Movement Disorders* 26.10 (2011), pp. 1859–1863.
- [7] Arash Salarian et al. “Quantification of tremor and bradykinesia in Parkinson’s disease using a novel ambulatory monitoring system”. In: *IEEE Transactions on Biomedical Engineering* 54.2 (2007), pp. 313–322.
- [8] Shyamal Patel et al. “Monitoring motor fluctuations in patients with Parkinson’s disease using wearable sensors”. In: *IEEE transactions on information technology in biomedicine* 13.6 (2009), pp. 864–873.

- [9] Dustin A. Heldman et al. “Automated motion sensor quantification of gait and lower extremity bradykinesia”. In: *Engineering in Medicine and Biology Society (EMBC), 2012 Annual International Conference of the IEEE*. IEEE. 2012, pp. 1956–1959.
- [10] Ji-Won Kim et al. “Analysis of lower limb bradykinesia in Parkinson’s disease patients”. In: *Geriatrics & gerontology international* 12.2 (2012), pp. 257–264.
- [11] Federico Parisi et al. “Body-sensor-network-based kinematic characterization and comparative outlook of UPDRS scoring in leg agility, sit-to-stand, and Gait tasks in Parkinson’s disease”. In: *IEEE journal of biomedical and health informatics* 19.6 (2015), pp. 1777–1793.
- [12] Joseph Jankovic. “Parkinson’s disease: clinical features and diagnosis”. In: *Journal of neurology, neurosurgery & psychiatry* 79.4 (2008), pp. 368–376.
- [13] James Parkinson. “An essay on the shaking palsy”. In: *The Journal of neuropsychiatry and clinical neurosciences* 14.2 (2002), pp. 223–236.
- [14] Karin Wirdefeldt et al. “Epidemiology and etiology of Parkinson’s disease: a review of the evidence”. In: *European journal of epidemiology* 26.1 (2011), p. 1.
- [15] Mark R. Cookson. “ α -Synuclein and neuronal cell death”. In: *Molecular neurodegeneration* 4.1 (2009), p. 9.
- [16] *Pesticides and Parkinson’s disease*. 2016. URL: <https://www.clinicaladvisor.com/features/link-between-pesticides-and-parkinsons-disease/article/492896/>.
- [17] *Understanding Parkinson’s disease*. URL: <https://www.mountnittany.org/articles/healthsheets/6889>.
- [18] Ahmed A Moustafa et al. “Motor symptoms in Parkinson’s disease: A unified framework”. In: *Neuroscience & Biobehavioral Reviews* 68 (2016), pp. 727–740.
- [19] Robert A. Hauser and Theresa A Zesiewicz. *Parkinson’s disease: Questions and Answers*. Merit, 2006.
- [20] Michelle E Fullard et al. “Olfactory impairment predicts cognitive decline in early Parkinson’s disease”. In: *Parkinsonism & related disorders* 25 (2016), pp. 45–51.
- [21] Emilia Iannilli et al. “Olfactory impairment in Parkinson’s disease is a consequence of central nervous system decline”. In: *Journal of neurology* 264.6 (2017), pp. 1236–1246.

- [22] Ronald F Pfeiffer. “Non-motor symptoms in Parkinson’s disease”. In: *Parkinsonism & related disorders* 22 (2016), S119–S122.
- [23] Qiu-Jin Yu et al. “Parkinson disease with constipation: clinical features and relevant factors”. In: *Scientific reports* 8.1 (2018), p. 567.
- [24] K Krogh et al. “Clinical aspects of bowel symptoms in Parkinson’s disease”. In: *Acta Neurologica Scandinavica* 117.1 (2008), pp. 60–64.
- [25] Matthew Menza et al. “Sleep disturbances in Parkinson’s disease”. In: *Movement Disorders* 25.S1 (2010), S117–S122.
- [26] Jyh-Gong Gabriel Hou and Eugene C Lai. “Non-motor symptoms of Parkinson’s disease”. In: *International Journal of Gerontology* 1.2 (2007), pp. 53–64.
- [27] Alfredo Berardelli et al. “Pathophysiology of bradykinesia in Parkinson’s disease”. In: *Brain* 124.11 (2001), pp. 2131–2146.
- [28] Hiram Houston Merritt. *Merritt’s neurology*. Lippincott Williams & Wilkins, 2010.
- [29] TC Booth et al. “The role of functional dopamine-transporter SPECT imaging in parkinsonian syndromes, part 1”. In: *American Journal of Neuroradiology* (2014).
- [30] Kimberly D. Seifert and Jonathan I Wiener. “The impact of DaTscan on the diagnosis and management of movement disorders: A retrospective study”. In: *American journal of neurodegenerative disease* 2.1 (2013), p. 29.
- [31] Jeffrey L. Cummings et al. “The role of dopaminergic imaging in patients with symptoms of dopaminergic system neurodegeneration”. In: *Brain* 134.11 (2011), pp. 3146–3166.
- [32] Barbara S. Connolly and Anthony E Lang. “Pharmacological treatment of Parkinson disease: a review”. In: *Jama* 311.16 (2014), pp. 1670–1683.
- [33] Robert A. Hauser. “How to dose carbidopa and levodopa extended-release capsules (Rytary)”. In: *Clinical Medicine* 1.2 (2015), pp. 34–37.
- [34] Lauren C. Seeberger and Robert A Hauser. “Carbidopa levodopa enteral suspension”. In: *Expert opinion on pharmacotherapy* 16.18 (2015), pp. 2807–2817.
- [35] Thomas Müller. “Catechol-O-methyltransferase inhibitors in Parkinson’s disease”. In: *Drugs* 75.2 (2015), pp. 157–174.

- [36] Rajesh Pahwa et al. “Amantadine extended release for levodopa-induced dyskinesia in Parkinson’s disease (EASED Study)”. In: *Movement Disorders* 30.6 (2015), pp. 788–795.
- [37] Janice M. Beitz. “Parkinson’s disease: a review”. In: *Front Biosci* 6 (2014), pp. 65–74.
- [38] Jeff M. Bronstein et al. “Deep brain stimulation for Parkinson disease: an expert consensus and review of key issues”. In: *Archives of neurology* 68.2 (2011), pp. 165–165.
- [39] Christopher G. Goetz et al. “Movement Disorder Society-sponsored revision of the Unified Parkinson’s Disease Rating Scale (MDS-UPDRS): Scale presentation and clinimetric testing results”. In: *Movement disorders* 23.15 (2008), pp. 2129–2170.
- [40] Errol Ozdalga, Ark Ozdalga, and Neera Ahuja. “The smartphone in medicine: a review of current and potential use among physicians and students”. In: *Journal of medical Internet research* 14.5 (2012).
- [41] Er Zainab Pirani et al. “Android based assistive toolkit for alzheimer”. In: *Procedia Computer Science* 79 (2016), pp. 143–151.
- [42] Hui Hsien Wu, Edward D Lemaire, and Natalie Baddour. “Change-of-state determination to recognize mobility activities using a Black-Berry smartphone”. In: *Engineering in Medicine and Biology Society, EMBC, 2011 Annual International Conference of the IEEE*. IEEE. 2011, pp. 5252–5255.
- [43] Beom-Chan Lee et al. “Cell phone based balance trainer”. In: *Journal of neuroengineering and rehabilitation* 9.1 (2012), p. 10.
- [44] Mohammad Ashfak Habib et al. “Smartphone-based solutions for fall detection and prevention: challenges and open issues”. In: *Sensors* 14.4 (2014), pp. 7181–7208.
- [45] Han Byul Kim et al. “Validation of freezing-of-gait monitoring using smartphone”. In: *Telemedicine and e-Health* (2018).
- [46] Gastone Ciuti et al. “MEMS sensor technologies for human centred applications in healthcare, physical activities, safety and environmental sensing: a review on research activities in Italy”. In: *Sensors* 15.3 (2015), pp. 6441–6468.
- [47] Michele Magno et al. “A low power wireless node for contact and contactless heart monitoring”. In: *Microelectronics Journal* 45.12 (2014), pp. 1656–1664.

- [48] Ming Liu. “A study of mobile sensing using smartphones”. In: *International Journal of Distributed Sensor Networks* 9.3 (2013), p. 272916.
- [49] Markos G. Tsipouras et al. “An automated methodology for levodopa-induced dyskinesia: assessment based on gyroscope and accelerometer signals”. In: *Artificial intelligence in medicine* 55.2 (2012), pp. 127–135.
- [50] Yves Kodratoff. *Introduction to machine learning*. Elsevier, 2014.
- [51] Marzyeh Ghassemi et al. “Opportunities in Machine Learning for Healthcare”. In: *arXiv preprint arXiv:1806.00388* (2018).
- [52] Hian Chye Koh, Gerald Tan, et al. “Data mining applications in healthcare”. In: *Journal of healthcare information management* 19.2 (2011), p. 65.
- [53] Jason Brownlee. “Supervised and unsupervised machine learning algorithms”. In: *Machine Learning Mastery* 16.03 (2016).
- [54] Ian Goodfellow et al. *Deep learning*. Vol. 1. MIT press Cambridge, 2016.
- [55] *Modern Machine Learning Algorithms: Strengths and Weaknesses*. URL: <https://elitedatascience.com/machine-learning-algorithms>.
- [56] Andrew R Webb. *Statistical pattern recognition*. John Wiley & Sons, 2003.
- [57] Jian Wu et al. “Mixed pattern matching-based traffic abnormal behavior recognition”. In: *The Scientific World Journal* 2014 (2014).
- [58] Mikel Galar et al. “An overview of ensemble methods for binary classifiers in multi-class problems: Experimental study on one-vs-one and one-vs-all schemes”. In: *Pattern Recognition* 44.8 (2011), pp. 1761–1776.
- [59] Bissan Ghaddar and Joe Naoum-Sawaya. “High dimensional data classification and feature selection using support vector machines”. In: *European Journal of Operational Research* 265.3 (2018), pp. 993–1004.
- [60] *Support Vector Machines*. URL: <https://amitranga.wordpress.com/machine-learning/support-vector-machines/>.
- [61] John J Hopfield. “Artificial neural networks”. In: *IEEE Circuits and Devices Magazine* 4.5 (1988), pp. 3–10.
- [62] S Agatonovic-Kustrin and R Beresford. “Basic concepts of artificial neural network (ANN) modeling and its application in pharmaceutical research”. In: *Journal of pharmaceutical and biomedical analysis* 22.5 (2000), pp. 717–727.

- [63] Daniel Shiffman. *The Nature of Code: Simulating Natural Systems with Processing*. Daniel Shiffman, 2012.
- [64] S Rasoul Safavian and David Landgrebe. “A survey of decision tree classifier methodology”. In: *IEEE transactions on systems, man, and cybernetics* 21.3 (1991), pp. 660–674.
- [65] *Decision tree Intuition*. 2010. URL: <https://medium.com/greyatom/decision-tree-intuition-a38669005cb7>.
- [66] J. Ross Quinlan. “Induction of decision trees”. In: *Machine learning* 1.1 (1986), pp. 81–106.
- [67] *How Decision Tree algorithm works*. 2017. URL: <http://dataaspirant.com/2017/01/30/how-decision-tree-algorithm-works/>.
- [68] Alan Julian Izenman. “Linear discriminant analysis”. In: *Modern multivariate statistical techniques*. Springer, 2013, pp. 237–280.
- [69] Petros Xanthopoulos, Panos M Pardalos, and Theodore B Trafalis. “Linear discriminant analysis”. In: *Robust data mining*. Springer, 2013, pp. 27–33.
- [70] Najla M Qarmalah, Jochen Einbeck, and Frank PA Coolen. “k-Boxplots for mixture data”. In: *Statistical papers* 59.2 (2018), pp. 513–528.
- [71] Olivier Caelen. “A Bayesian interpretation of the confusion matrix”. In: *Annals of Mathematics and Artificial Intelligence* 81.3-4 (2017), pp. 429–450.